Short title: Adaptive homeostasis to drought in Arabidopsis

Adaptive growth homeostasis in response to drought in Iberian Arabidopsis accessions

Ángel Ferrero-Serrano[1] & Sarah M. Assmann[1]

[1]Biology Department, Penn State University, 208 Mueller Laboratory, University Park, PA, 16802, USA

One-sentence summary: Information on phenotype, genotype, and transcript abundance is integrated to identify both plasticity and homeostasis genes and processes associated with local adaptation to drought stress in Arabidopsis accessions of the Iberian Peninsula.

Author contributions: S.M.A & A.F-S. conceived the project, research plans and experimental design. A.F-S. performed the experiments while S.M.A provided guidance throughout the experimental work. A.F-S. analyzed the data and prepared the figures; S.M.A provided supervision with data analysis and figure preparation. S.M.A & A.F-S wrote the manuscript. A.F-S agrees to serve as the author responsible for contact and ensuring communication and assistance with the reproducibility of the results of this study.

ABSTRACT

Plants respond to environmental fluctuations through plastic phenotypic shifts. Whether a plastic response upon environmental variability is adaptive or not has been subject to debate. Using a set of Iberian Arabidopsis accessions, we quantified an interplay between passive plastic reductions in leaf areas that we found typical of accessions from productive environments and homeostatic leaf areas responses to drought typified by accessions originating from unproductive environments. Results from Genome-Wide Association Studies (GWAS) and Transcriptome Wide Association Studies (TWAS) highlight the role of auxin-related processes and, in particular, the possible role of the *SMALL AUXIN UP RNA 26* (*SAUR26*) gene in the regulation of the observed plastic responses. Homeostatic responses in leaf area potential following drought were typical of accessions with lower leaf area potential under well-watered conditions. Transcripts that were negatively associated with leaf area potential and positively associated with homeostatic and positive leaf area plasticity following drought showed functional enrichment in ion transport processes. We hypothesized that the contrasting plastic and homeostatic responses in leaf area potential were associated with differential intrinsic water use efficiency (WUE_i). We confirmed this relationship in a metanalysis conducted using previously published $\delta^{13}C$ measurements. Our results highlight the adaptive role of homeostatic leaf area response to water depletion arising from increased WUE_i. The concerted utilization of Genome-Wide Association Studies (GWAS), Transcriptome Wide Association Studies (TWAS), and expression Genome-Wide Association Studies (eGWAS) allows integration of phenotype, genotype, and transcript abundance to identify both "plasticity genes" and "homeostasis genes" associated with drought stress responses.

INTRODUCTION

Earth is undergoing a climate change scenario resulting in extreme weather events that are increasingly frequent and variable (Easterling et al., 2000; Meehl and Tebaldi, 2004; Schär et al., 2004). These changing conditions are creating opportunities for some species to spread beyond their native ranges (Chen et al., 2011) while posing a challenge to species that are currently adapted to their local environment (Holt, 1990). As sessile organisms, plants must complete their life cycle in their local environment and consequently are experiencing changing climate conditions at an increasing rate and severity. A developmentally plastic response (West-Eberhard, 2003) is accepted as an appropriate response to environmental change during the lifetime of an individual plant. However, simply because a given trait is plastic does not mean that this plasticity is adaptive (Ghalambor et al., 2007). Active plasticity is anticipatory in response to predictable environmental cues. On the other hand, passive plasticity is not anticipatory but a consequence, often proportional, to a resource limitation. Active plastic phenotypic responses to environmental cues are thus more likely to be adaptive than passive plasticity that unavoidably arises from unpredictable resource limitation (Dorn et al., 2000; van Kleunen and Fischer, 2005; Forsman, 2015). However, the division

between passive and active plasticity is not straightforward. It not only depends on whether the environmental factor is a reliable cue such as daylength or an unpredictable resource such as water (precipitation) but also on the phenotype under consideration. For example, when plants are subjected to drought, their growth is limited, a passive response. Still, they can also respond actively by accelerating the onset of the reproductive stage (early flowering time).

The study of passive plastic responses to changes in resource availability can provide insights into plant responses to climate change-related events that are unpredictable. Water availability is indeed unpredictable, as the frequency and intensity of precipitation vary seasonally, annually, and geographically (Loik et al., 2004). Drought is thus among the strongest factors driving adaptation in plants (Siepielski et al., 2017; Exposito-Alonso et al., 2019). Climate projections for the remainder of the 21st century predict precipitation extremes to become more severe (Donat et al., 2016) and for this reason, understanding the genetic basis and adaptation potential of phenotypic traits and their plastic or homeostatic responses to drought is paramount.

Water availability ranges in a continuum from critically low to abundant and even excessive. The distribution of phenotypic traits and their plasticity in a population is often continuous (Galton, 1894) because they are influenced by variation in a large number of genes. The effect of many of these variants is additive or synergistic and of small effect individually (Fisher, 1919), and thus difficult to identify (Barton et al., 2019; Sohail et al., 2019). For example, leaf area displays natural intraspecific variation and varies in a continuous manner in response to resource availability. Leaf area is an important trait in relation to carbon and water fluxes: the degree of growth and leaf area production is indicative of the total amount of light intercepted by plants, assimilated carbon, but also evaporative water loss. Leaf area response to drought is not only of interest from an ecological perspective; for instance, biofuel production from non-grain biomass depends on vegetative growth (Varvel et al., 2008; Pols and Spahn, 2014).

The Iberian Peninsula is a drought-prone region particularly vulnerable to climate change effects on precipitation (Vicente-Serrano, 2006a; Vicente-Serrano, 2006b; Coll et al., 2016; Páscoa et al., 2017). The Iberian Arabidopsis population is particularly valuable because its accessions originate from a broad range of environments (Lobo et al., 2001; Rey Benayas and Scheiner, 2002). These accessions represent the region in continental Europe with the highest genetic diversity in Arabidopsis (Cao et al., 2011; The 1001 Genomes Consortium, 2016). The population structure of the Iberian accessions is well-defined (Picó et al., 2008; The 1001 Genomes Consortium, 2016), and previous studies in the Iberian population have provided considerable insight into the evolution and development of Arabidopsis (Picó et al., 2008; Montesinos et al., 2009; Gomaa et al., 2011; Méndez-Vigo et al., 2011; Montesinos-Navarro et al., 2011; Picó, 2012; Manzano-Piedras et al., 2014; Wolfe and Tonsor, 2014; Vidigal et al., 2016; Exposito-Alonso et al., 2018a; Marcer et al., 2018).

Natural populations of Arabidopsis, including those of the Iberian Peninsula, constitute an important component of the 1001 Genomes Project (The 1001 Genomes Consortium, 2016). The Arabidopsis 1001 Genomes Project provides high-quality full genome information for 1,135 inbred accessions collected from geolocated sites across an extensive distribution range, with a well-studied population history (The 1001 Genomes Consortium, 2016; Durvasula et al., 2017), and well-

119 characterized local environments (Ferrero-Serrano and Assmann, 2019). In addition, a reference
120 panel is available with transcript abundance data for 727 Arabidopsis accessions (Kawakatsu et al.,
121 2016), including 665 accessions that overlap with the collection of accessions included in the 1001
122 Genomes project (The 1001 Genomes Consortium, 2016); 189 of the 1,135 accessions are from the
123 Iberian peninsula. This information provides the tools needed to study the genetic basis of phenotypic
124 potential (i.e., the normalized maximum phenotypic value) and its plastic responses to a limiting
125 resource such as drought.
126 In addition to GWAS, natural variation in abiotic stress-responsive transcript abundance can
127 identify adaptive mechanisms (Des Marais et al., 2012; Lasky et al., 2014). Transcriptome Wide
128 Association Studies (TWAS) associate transcript abundance with phenotypic traits (Gusev et al.,
129 2016; Kremling et al., 2019), while eGWAS identifies candidate SNPs (expression SNPs or eSNPs)
130 that control transcript abundance. Here, we utilize GWAS, TWAS, and eGWAS to identify the
131 natural genetic and transcript abundance variation underlying both plastic and homeostatic responses
132 to drought. We uncover an adaptive homeostatic growth strategy in accessions from less productive
133 environments, dissect its genetic basis, and conclude that, just as has been argued previously for
134 plasticity, homeostasis is under genetic control and of evolutionary importance.

135 **RESULTS**

136 **Natural variation in leaf area and plasticity in response to long-term drought**

137

138 To quantify phenotypic variation in Iberian Arabidopsis accessions exposed to sustained drought, we
139 conducted a common garden experiment (Fig. 1A). We used image analysis to derive rosette leaf area
140 for 43 Iberian accessions grown under well-watered or drought conditions (Fig. 1B, C; Table P1). As
141 expected, we observed a reduction in leaf area resulting from drought in most genotypes, as evident
142 from the phenotypic reaction norms, while a small number of accessions exhibited constant or
143 increased leaf area under drought (Fig. 1A,D,E). Based on these data, we calculated leaf area
144 potentials (Fig.1B,C,S,E) and plasticity indexes. We define leaf area potential as the normalized
145 maximum phenotypic value realized by any given accession under each condition of the experiment
146 (well-watered or drought). We used potential rather than actual values in order to allow comparison
147 of relative leaf area of each accession within the study population between both watering regimes.
148 A leaf area plasticity index was calculated (Bouslama and Schapaugh, 1984) for each
149 accession based on the difference in leaf area potential between drought and well-watered conditions,
150 i.e., based on the reaction norms in Fig. 1F; Table P1. Genetic variants significantly associated with
151 this parameter were identified by GWAS (Fig. 2A; Table G3). Gene ontology (GO) analysis of
152 functions associated with the genes harboring the variants identified by GWAS revealed an
153 enrichment in auxin-related functions (Fig. 2A; Table GO3). Among the variants identified from
154 GWAS (Fig. 2A; Table G3) and TWAS (Table T1,T2) as associated with leaf area plasticity, we
155 highlight two co-varying SNPs in the 5' and 3' UTR of *SMALL AUXIN UP RNA 26* (*SAUR26*,

156 AT3G03850**)** (Figure 2B). We also found from eGWAS that the transcript levels of *SAUR26* are
157 regulated by this genetic variation (cis-regulation; Fig. 2C; Table G6).
158 We illustrate the haplotypic differences in leaf area plasticity for *SAUR26* that we identify in
159 our study (Figure 2B). Accessions harboring the minor *SAUR26* haplotype display negative plasticity
160 in leaf area while the major haplotype is associated with homeostatic and positive plasticity responses
161 in leaf area in response to drought (Fig. 2D; Wilcoxon *P*-value < 0.001). These haplotypic differences
162 were also associated with the transcript levels of *SAUR26* (Figure 2C), which we confirmed both in
163 the group of accessions included in our study (Wilcoxon *P*-value < 0.001) as well as in the 189 Iberian
164 accessions included within the 1001 Genomes Project (Fig. 2E; Wilcoxon *P*-value < 0.001). Both the
165 genetic variation defined by this haplotype in *SAUR26* and the resulting transcript abundance are
166 associated with the interplay between plasticity and homeostasis that we define in our study (Fig.
167 2D,F). These results highlight *SAUR26* as a candidate regulator of leaf area plasticity in response to
168 drought (Fig. 2G).
169 We conducted a GWA analysis of leaf area potential based on the genome-wide association
170 of individual SNPs for leaf area in response to drought (Fig. S1A, Table G1, G2). In our GWA
171 analysis on leaf area potential (Fig. S1A, Table G1, G2), no SNPs were found that were associated
172 with leaf area potential under both well-watered and drought conditions, i.e., no SNPs that would be
173 depicted as horizontal lines in Fig. S1A. The results from TWA analysis were strikingly different,
174 identifying transcripts associated with both leaf area plasticity (Fig. S1B) and leaf area homeostasis
175 (Fig. 3). A TWA analysis identified five transcripts that are positively correlated with leaf area
176 potential under both well-watered and drought conditions: *SOFL2*, *CPN60B*, *AT5G02244*, *CKL8*, and
177 *IBH1* (Fig. 3A). This means that accessions with higher transcript abundance of these genes display
178 higher leaf area potential under both well-watered and drought conditions. We highlight *IBH1* as an
179 example (Fig. 3B). Conversely, we identified four genes negatively correlated with leaf area potential
180 such that accessions with a higher transcript abundance display lower leaf area potentials under both
181 well-watered and drought conditions: *RHF1A*, *AT5G60160*, *AT4G15260*, and *AT5G16800* (Fig. 3A).
182 We highlight *RHF1A* as an example (Fig. 3C).
183

184 Trade-off between growth, plasticity and intrinsic water use efficiency

185

186 We determined that the plastic leaf area responses we observed in our study were typical of accessions
187 from more productive habitats, while homeostatic responses were typical of accessions from less
188 productive habitats (Fig. S2). We next explored the relationship between leaf area potential in the
189 absence of drought and its plastic response when drought is imposed. In Figure 4A, orange points
190 depict accessions that display a reduction in leaf area in response to drought (negative plasticity) but
191 that in the absence of drought display a high leaf area potential. Blue datapoints represent those
192 accessions with homeostatic or positive growth responses to drought and low leaf area potential under
193 well-watered conditions. Red points are accessions with negative plastic responses and low
194 phenotypic potential. Finally, green datapoints are those accessions displaying homeostatic or
195 positive responses to drought that exhibit relatively high leaf areas in the absence of drought. We

196 observe a trade-off between growth, indicated by high leaf area potential in the absence of drought,
197 and leaf area homeostasis in response to drought. Accessions with higher leaf area potential displayed
198 higher plastic reductions in leaf area potential when subjected to drought. On the contrary, accessions
199 with lower leaf area potential under well-watered conditions display homeostatic phenotypic
200 responses to drought (Fig. 4A).

201 We performed a GWA analysis (Fig. 4B; Table G1,G3) to determine the genetic basis of the
202 trade-off between growth and homeostasis in response to drought illustrated in Fig. 4A. The green
203 datapoints (representing four different genes) are those significantly associated with both leaf area
204 potential and plasticity index and thus are candidate regulators of the trade-off. Among the candidate
205 variants, we identified two co-varying SNPs in *PR5K-LIKE RECEPTOR KINASE* (*PR5K,*
206 *AT5G38280*). The role of *PR5K* in drought and growth processes is not known, but another *PR5K-*
207 *LIKE RECEPTOR*, *PR5K2,* is a key negative regulator of ABA signaling via phosphorylation of
208 PP2C phosphatases such as *ABI1* and *ABI2* (Baek et al., 2019). We also identified two non-co-varying
209 SNPs in *RAP2.7* as potential regulators of the trade-off between leaf area potential and plasticity.
210 *RAP2.7* is part of the AP2 family of transcription factors, and we would expect it to be involved in
211 flowering time processes (Du et al., 2020) rather than growth and plastic leaf area growth responses
212 to drought. *WRKY DNA-binding protein 51* (*WRKY51*, *AT5G64810*) has been previously linked to
213 defense responses (Gao et al., 2011) but not to drought, leaf area, or plasticity. Finally, the function
214 of *AT5G16990* has not been previously characterized. Gene Ontology analysis on the 17 genes that
215 include the 50 SNPs with the strongest association with leaf area potential reveal an enrichment in
216 responses to osmotic and salt stress (Table GO3). This will become relevant to the tradeoff between
217 growth and plasticity as shown by our analysis of this process using TWAS, described below.

218 Figure 4C depicts the relationship between transcript abundance and the observed trade-off
219 between growth and homeostasis in response to drought (Table T1,T2). Orange datapoints in Fig. 4C
220 are transcripts with higher abundance in those accessions that are plastic and display higher leaf area
221 potentials under well-watered conditions (depicted in orange in Fig. 4A). Conversely, blue points in
222 Fig. 4C are transcripts with higher abundance in those accessions that are homeostatic and display
223 lower leaf area potentials under well-watered conditions (depicted in blue in Fig. 4A). Gene Ontology
224 analysis reveals that the transcripts negatively associated with leaf area potential are involved in ion
225 transmembrane processes (Table GO3). This enrichment is also confirmed in the 30 transcripts
226 depicted as blue datapoints in Fig. 4C (Table GO5).

227 A relationship between $\delta^{13}C$ and intrinsic water use efficiency has been confirmed in natural
228 populations of Arabidopsis (Juenger et al., 2005; Easlon et al., 2014). Following this, we analyzed
229 the $\delta^{13}C$ values recorded by Dittberner et al. (2018), available for 21 of the accessions used in our
230 study. The results revealed a trade-off between plasticity and WUE_i (Fig. 4D). Accessions that exhibit
231 strong negative plasticity in the presence of drought have a lower intrinsic water use efficiency in the
232 absence of drought (more negative $\delta^{13}C$ values). Those accessions that maintain leaf area in response
233 to drought display a higher water use efficiency in the absence of drought (more positive $\delta^{13}C$ values).

234 We found no genetic variants associated with the observed trade-off between intrinsic water
235 use efficiency and leaf area plasticity in response to drought (Fig. 4E; Table T1,T2), i.e., no datapoints

236 in the upper right quadrant of Fig. 4E. However, TWA analysis (Table S2) provided insight into this
237 trade-off. Red datapoints in Fig. 5F are transcripts with higher greater abundance in those plastic and
238 less water-use efficient accessions depicted in red in Fig. 4D. Conversely, green points in Fig. 4F
239 represent transcripts with greater abundance in the homeostatic and water-use efficient accessions
240 depicted in green in Fig. 4D. GO analysis revealed an enrichment in snRNA and rRNA pseudouridine
241 synthesis (Table GO7) for transcripts that display higher abundance in accessions with high negative
242 plastic responses and lower WUE_i (red datapoints in 4F). We chose *CNGC16* and *AHA4* (see
243 Discussion) to exemplify transcripts with opposed relationships to leaf area plasticity and water use
244 efficiency (Fig. 5).
245

246 ## Intrinsic water use efficiency in the Iberian population

247

248 We determined that in our study, accessions that displayed positive growth or homeostasis in leaf
249 area in response to drought (Fig 4A) also had higher WUE_i in the absence of drought (Fig. 4D). We
250 then conducted a meta-analysis on the 95 Iberian accessions with $\delta^{13}C$ information from a previous
251 study focused on the global Arabidopsis population (Dittberner et al., 2018). GWA analysis of these
252 accessions rendered a distinctive peak in a single gene, identifying a haplotype consisting of eight co-
253 varying SNPs in *ClpX3* (*AT1G33360*; Fig. 6A; Table G5), an ATP-dependent Clp protease. More
254 informative was the TWA analysis of water use efficiency determined from ($\delta^{13}C$) values in the 88
255 Iberian accessions with both published transcript abundance and $\delta^{13}C$ information: we uncovered a
256 distinctive enrichment in photosynthesis-related genes (Table. GO8) in transcripts that are
257 upregulated in accessions with high water use efficiency (more positive $\delta^{13}C$ values; Fig. 6B; Fig.
258 S4; Table T1,T2). We highlight the positive relationships uncovered for the transcript abundance of
259 *RuBisCO small subunit 2B* (*AT5G38420*; *RBCS2B;* Fig. 6C), *PLASMA MEMBRANE INTRINSIC*
260 *PROTEIN 1;5* (*AT4G23400*; *PIP1;5*; Fig. 6D) with WUE_i. Finally, we highlight the positive
261 relationship between the transcript abundance of *SAUR26* and WUE_i (Fig. 6E), in concordance with
262 the findings of our study.
263

264 # DISCUSSION

265

266 ## Identifying candidate regulators of passive plasticity and adaptive homeostasis

267

268 There is an adaptive trade-off between growth and drought resistance in plants (Zhang et al., 2020).
269 Plants adapted to more productive habitats with higher and more constant precipitation regimes favor
270 decreased water use efficiency and increased carbon capture, producing increased leaf areas to
271 compete for aboveground resources with neighbors (Tilman, 1988). Conversely, plants adapted to
272 unproductive environments typically fix less carbon, have higher water use efficiency, and display
273 low growth rates, even when grown in rich environments (Parsons, 1968; Chapin, 1991), and are
274 typical stress-tolerant (Billings and Mooney, 1968; Grime, 1977). In this study, we observe that
275 accessions with higher leaf area potentials in the absence of drought display strong and negative

276 plastic responses to drought (Fig. 1). On the other hand, accessions with lower leaf area potential in
277 the absence of drought exhibit leaf area homeostasis or even positive leaf area potential plastic
278 responses in response to drought (Fig. 1,4A).

279 Natural variation in the degree of plasticity among different ecotypes (accessions in the case
280 of Arabidopsis) that are subjected to similar depletions in water availability can provide valuable
281 information on the adaptive/neutral/maladaptive role of this plastic response. The variation in leaf
282 area in Arabidopsis accessions in response to drought in this study can be grossly divided into passive
283 and negative phenotypic plasticity in accessions adapted to richer environments (high Net Primary
284 Productivity in spring, NPP spring), vs. adaptive phenotypic homeostasis responses observed in
285 accessions originating from less productive areas of the Iberian Peninsula (low NPP spring) (Fig. S2).
286 We sought to identify the genetic basis of these contrasting ecological strategies.

287 Identifying causal genetic variants related to an abiotic stress response such as drought is
288 challenging given the polygenic nature of these responses (Exposito-Alonso et al., 2018b). Moreover,
289 here, our main interest was not to identify natural variation associated with well-watered or drought
290 phenotypes, but rather natural variation associated with the degree of plasticity evoked in response to
291 drought, i.e., natural variation associated with reaction norms, rather than with phenotypes in one
292 environment or the other (well-watered or drought). Reaction norms in leaf area in response to
293 drought (Fig. 1E, F) illustrate the plasticity index that we calculated based on the difference in leaf
294 area potential between drought and well-watered conditions (Table P1). In exploring the genetic basis
295 of plasticity, we identified the 31 genes corresponding to the top 50 candidate SNPs with the highest
296 strength of association with the leaf area plasticity index that we calculated (Figure 2B; Table G3).
297 Of these 31 genes, 20 have been previously characterized, and many of these are related to auxin
298 regulation and leaf expansion. This enrichment in auxin-related processes was confirmed by GO
299 analysis (Table GO3). The variant with the strongest association with the plastic response to drought
300 was the auxin efflux carrier family protein *PIN8* (*AT5G15100*). The SNPs with the third and fourth-
301 highest scores (strength of association) correspond to co-varying variants in *AUXIN RESPONSE*
302 *FACTOR 16* (*ARF16*; *AT4G30080)*. Among the candidates, we also obtained two co-varying SNPs
303 in *SMALL AUXIN UP RNA 26* (*SAUR26*; *AT3G03850*); two variants in *AGAMOUS-like 15*
304 (*AT5G13790*; *AGL15*), a gene that negatively regulates auxin signaling in Arabidopsis (Zheng et al.,
305 2016); and three variants in *LONESOME HIGHWAY LIKE 1* (*LL2*; *AT2G31280*), an atypical basic
306 helix-loop-helix (bHLH) transcription factor known to regulate early xylem development
307 downstream of auxin (Ohashi-Ito et al., 2013). Among the candidates that are not included in the GO
308 category "response to auxin", we find four co-varying SNPs in the *Basic helix-loop-helix (bHLH)*
309 *DNA-binding family protein MYC3* (AT5G46760), a known regulator of glucosinolate biosynthesis
310 (Schweizer et al., 2013). Auxin negatively regulates glucosinolate levels, and this regulation appears
311 to integrate growth and stomatal regulation during drought (Salehin et al., 2019). TWAS analysis
312 also revealed associations with auxin through glucosinolate biosynthesis: GO biological process
313 analysis on positively correlated candidates resulting from TWAS analysis on leaf area plasticity
314 index for drought revealed an enrichment of glucosinolate biosynthesis genes (Table S6).

315 We found that among the auxin-related variants associated with leaf area plasticity (Fig. 2A),
316 SNPs in *SAUR26* were of particular interest. The majority of characterized *SAUR* genes are positive
317 regulators of plant growth (Spartz et al., 2014; Li et al., 2015; Stortenbeker and Bemer, 2019). The
318 two associated variants in *SAUR26* were found in the 5' and 3' UTR, respectively (Fig. 2B), regions
319 of the ORF that typically regulate gene expression. Indeed, we found the transcript levels of *SAUR26*
320 to be associated with the genetic variation in *SAUR26* itself (cis-regulation; Fig. 2C), which we
321 confirmed both in the group of accessions included in this study and in the 189 Iberian accessions
322 included within the 1001 Genomes Project (Fig. 4E). The minor haplotype is associated with negative
323 plasticity in leaf area in response to drought. Conversely, the major haplotype, associated with higher
324 transcript abundance of *SAUR26*, is associated with leaf area homeostasis and positive plastic
325 responses (Fig. 2D).
326 Relevant to the non-discrete distribution of the plastic responses in the accessions that we
327 studied, variation in transcript abundance of *SAUR26* explained 17% of the observed plastic response
328 in leaf area to drought in our study (Figure 2F, G). The importance of *SAUR26* is supported by
329 previous work that revealed natural genetic variation in *SAUR26* associated with growth thermo-
330 responsiveness of the rosette compactness index (Wang et al., 2019) and cis-elements in the 5'
331 upstream region or the 3'UTR region of *SAUR26* that were responsible for this response (Wang et al.
332 2021). This conclusion is also supported by our meta-analysis of the larger Iberian population with
333 transcriptome data, which also identified *SAUR26* transcript abundance as positively correlated with
334 higher water use efficiency (Fig. 6B,C) along with other related auxin-related transcripts such as
335 *AUXIN RESISTANT 3* (*AXR3*, also known as *IAA17*, *AT1G04250*) (Leyser et al., 1996) and *SMALL*
336 *AUXIN UPREGULATED 15* (*SAUR15*, *AT4G38850*) (Oh et al., 2014) (Fig. 6B). As we uncover in
337 this study, both transcript abundance and natural genetic variation in *SAUR26* cis-regulatory elements
338 are associated with the interplay between plasticity and homeostasis in leaf area potential following
339 drought stress (Fig. 2, Table G3,T1,T2). Interestingly, the minor haplotype frequency for this
340 haplotypic variant in our study sample (Minor haplotypic frequency, MHF = 38.09%) has a frequency
341 similar to the frequencies we find in the 189 accessions within the Iberian population (MHF = 35.98).
342 However, the minor haplotype in the Iberian population becomes the haplotype in higher frequency
343 (64.14%) in the global 1001 Genomes collection. We know that Iberian Arabidopsis populations
344 locally adapted to drought conditions in this region out-perform accessions from wetter areas of
345 Northern Europe when both are exposed to drought (Exposito-Alonso et al., 2019). Following this,
346 given that the major haplotype in our study is associated with homeostatic responses to drought (Fig.
347 2D), and that its frequency became less frequent outside the drought-prone Iberian region, we can
348 speculate that this *SAUR26* haplotypic variant is under selection in the Iberian population conferring
349 an adaptive advantage to water-limited conditions in the region.
350 The study of the strength of association of genetic variation with leaf area plasticity provides
351 us with candidates that reveal a binary answer: one allele is associated with plastic reductions in leaf
352 area while the alternative allele will display an association with either homeostatic or positive
353 plasticity (increase in leaf area potential) under drought. We did not identify any SNPs associated
354 with leaf area potential under both well-watered and drought conditions. Therefore, we could not

355 define the genetic basis of growth homeostasis under drought using GWAS (Fig. S1). On the other
356 hand, reaction norms based on the strength of association of transcript abundance with leaf area
357 potential identify five transcripts that are positively correlated with leaf area potential under both
358 well-watered and drought conditions (Fig. 3A). This means that accessions with higher transcript
359 abundance for those genes display higher leaf area potential under both well-watered and drought
360 conditions. Conversely, we identified four transcripts negatively correlated with leaf area potential
361 such that accessions with a higher transcript abundance of those genes display lower leaf area
362 potentials under both well-watered and drought conditions. Therefore, these nine genes are strong
363 functional candidates for homeostatic regulation of leaf area potential.
364 Most of the candidate genes we obtained from this analysis have not been characterized, and
365 for those that have, their function is not necessarily known to be involved in growth processes leading
366 to differential leaf area. Among the homeostatic transcripts positively correlated with leaf area
367 potential, *ILI1 binding bHLH 1* (*IBH1,* AT2G43060) (Fig. 3B) has been previously shown to improve
368 drought tolerance in Arabidopsis (Moreno et al., 2018) which is consistent with the homeostatic
369 response that we observe. At the same time, ectopically expressed *IBH1* represses cell elongation in
370 Arabidopsis (Ikeda et al., 2012; Zhiponova et al., 2014), and expression of Arabidopsis *IBH1* in
371 transgenic tobacco plants (*Nicotiana tabacum*) induces a dwarf phenotype (Nagatoshi et al., 2016).
372 In our study, we observe a direct relationship between the natural variation in the transcript abundance
373 of *IBH1* and leaf area potential, which seems counterintuitive based on these latter reports, perhaps
374 reflecting an interaction between genotypic background and *IBH1*. *SOFL2* (Fig. 3C), another
375 candidate positively correlated with leaf area potential and homeostasis. has been previously reported
376 to confer an increase in the levels of specific cytokinins, which positively regulate plant growth
377 (Zhang et al., 2009). From inspection of the four candidate homeostatic transcripts that are negatively
378 correlated with leaf area potential, only *RING-H2 GROUP F1A* (*RHF1A*; *AT4G14220*) has been
379 previously characterized. While the role of *RHF1A* in the regulation of leaf growth has not been
380 studied, it directly interacts with *KIP-related protein 6* (*KRP6*; *AT3G19150*) (Liu et al., 2008). The
381 overexpression of *KRP* genes reduces cell proliferation by inhibiting CDKs, resulting in small plants
382 with large cells (De Veylder et al., 2001). We can hypothesize that higher transcript abundance of
383 *RHF1A* may result in reduced vegetative growth by interacting with *KRP* genes.
384

385 To increase leaf area potential and sacrifice WUE_i or increase WUE_i and sacrifice 386 leaf area potential?

387

388 We found that accessions with higher leaf area potential displayed greater plastic reductions in leaf
389 area potential (negative leaf area plasticity index) when subjected to drought (Fig. 4A). This response
390 is presumably neither adaptive nor maladaptive but a consequence or passive response to a limited
391 resource rather than an active response. Consistent with this, accessions with plastic responses are
392 typical of productive habitats, while the homeostatic responses that we observed in our study typify
393 accessions collected from less productive habitats (Fig. S2).

394 Gene Ontology analysis on the 17 genes that include the 50 SNPs with the strongest
395 association with leaf area potential (green and yellow datapoints in Fig. 4B) reveals an enrichment in
396 responses to osmotic and salt stress (Table GO1). Gene Ontology analysis also reveals that the
397 transcripts negatively associated with leaf area potential are involved in ion transmembrane processes
398 (Table GO2). This enrichment is also confirmed in the 30 transcripts depicted as blue datapoints in
399 Fig. 4C (Table GO5). We hypothesized that these processes are related to the greater water use
400 efficiency of accessions with reduced growth rates typical of unproductive environments. Indeed,
401 plant species with low relative growth rates are known to exhibit high intrinsic water use efficiency
402 (WUE_i) (Angert et al., 2009; Kimball et al., 2012). WUE_i is defined as the ratio between instantaneous
403 carbon gain and transpirational water loss, typically calculated per unit of leaf area (Condon et al.,
404 2002). In support of our hypothesis, the homeostatic response in leaf area potential in response to
405 prolonged drought that we observe in our study correlates positively with a high predicted water use
406 efficiency recorded by Dittberner et al. (2018) for the same accessions (Fig. 4D). While we regard
407 the observed plasticity in response to drought as a passive response to resource availability, we
408 propose that the observed leaf area homeostasis is an adaptive response.
409 These observations are consistent with what has been described before in classic ecological
410 studies, as well as in studies on crop cultivars (Kasuga et al., 1999; Ferrero-Serrano and Assmann,
411 2016; Ferrero-Serrano et al., 2018). There were no overlapping SNPs associated with both the leaf
412 area plasticity index and WUE_i (Fig. 4E). However, when we compare the candidates obtained from
413 TWAS analysis, we identify transcripts associated with both low WUE_i and a negative plastic
414 response in leaf area when subjected to sustained drought. Conversely, we identify a set of transcripts
415 that is significantly associated with both leaf area homeostasis (more positive leaf area plasticity
416 index) and increased WUE_i (Fig. 4F). To exemplify these opposed responses to drought, given the
417 enrichment in ion transport genes that we found in the transcripts regulating the tradeoff between leaf
418 area plasticity and potential (Fig. 4C; Table GO5), we highlight two of the genes identified by TWAS,
419 with opposite correlations between transcript abundance and relative leaf area plasticity (Fig. 6A,B
420 vs. Fig. 6C,D): *CYCLIC NUCLEOTIDE GATED CHANNEL 16* (*CNGC16*; *AT3G48010*) and Plasma
421 Membrane H^+ ATPase 4 (*AHA4*; *AT3G47950*).
422 CNGCs are a superfamily of cation channels permeable to divalent and monovalent cations,
423 including Ca^{2+} and K^+ (Köhler et al., 1999; DeFalco et al., 2016). *CNGC*s like *CNGC5* and *CNGC6*
424 have been previously reported to be required for a cyclic GMP (cGMP)-activated nonselective Ca^{2+}-
425 permeable cation channel activity in the plasma membrane of Arabidopsis guard cells (Wang et al.,
426 2013) associated with stomatal closure. In particular, *CNGC16* is critical for reproductive success
427 following drought stress (Tunc-Ozdemir et al., 2013). Consistent with these functional roles, in our
428 study, higher transcript abundance of *CNGC16* is found in accessions with positive leaf area plasticity
429 indexes under drought (leaf area homeostasis; Fig. 5A); and with high WUE_i (Fig. 5B).
430 The inverse relationship is found for the transcript abundance of *AHA4*. Auxin-mediated
431 signaling and growth involve the activation of plasma membrane H^+ ATPases (Hager, 2003; Rober-
432 Kleber et al., 2003; Takahashi et al., 2012), and activation of H^+ ATPases also drive stomatal opening,
433 which results in decreased WUE_i. This is supported by the negative correlation between leaf plasticity

434 and *AHA4* transcript abundance that we observe, wherein accessions with higher transcript abundance
435 of *AHA4* display strong negative plastic responses in leaf area potential in response to drought (Fig.
436 5C). Accordingly, the increased transcript abundance of *AHA4* is also associated with reduced WUE_i
437 (Fig. 5D).
438 We have described two opposed processes in response to sustained drought. On the one hand,
439 accessions displaying higher leaf area potential in the absence of drought display a higher plastic
440 reduction in leaf area potential following drought than accessions with lower leaf area potential in the
441 absence of drought. Indeed, species with high relative growth rates are known to exhibit low WUE_i
442 (Angert et al., 2009; Kimball et al., 2012). We argue that accessions from less productive
443 environments in the Iberian Arabidopsis population are adapted to drought and maintain homeostatic
444 response in leaf area to drought through their increased intrinsic water use efficiency.
445 Given the increased plastic responses in leaf area that we found in accessions with lower water
446 use efficiency, we next conducted a meta-analysis on the larger set of 95 Iberian accessions with $\delta^{13}C$
447 information from a previous study focused on the global Arabidopsis population (Dittberner et al.,
448 2018). Upon inspection of the candidates obtained from GWAS analysis of $\delta^{13}C$ values in Iberian
449 accessions, we could not identify an overarching functional theme, neither from GO biological
450 process analysis nor from published studies of the genes in which the associated variants were located.
451 However, we obtained a distinctive peak consisting of eight co-varying SNPs in a single gene, *ClpX3*
452 (*AT1G33360*; Fig. 6A), an ATP-dependent Clp protease. The Clp protease system is a central
453 component of the plastid protease network, ensuring the removal of aggregated and misfolded
454 proteins (Nishimura and van Wijk, 2015). *Clp* core mutants *clpr2* and *clpr4* null mutants display a
455 remarkable loss of chlorophyll (95 to 98% reduction) and photosynthetic capacity, turning entirely
456 white when grown under high light (Kim et al., 2009). The *clpr4-1* mutant displays a downregulation
457 of photosynthetic thylakoid proteins, the cytb_6f complex, the ATP-synthase, and the NDH complex,
458 as well as stromal *RuBisCO* large and small subunits, and allene oxide synthase (Kim et al., 2009).
459 We conducted TWAS analysis of WUE_i determined from $\delta^{13}C$ values in the 88 Iberian
460 accessions with both $\delta^{13}C$ information (Dittberner et al., 2018) and published transcript abundance
461 (Kawakatsu et al., 2016). Gene Ontology (GO) biological process analysis on the resultant 45
462 candidates positively correlated with $\delta^{13}C$ uncovered an unequivocal enrichment in photosynthesis-
463 related genes for transcripts that are upregulated in accessions with high WUE_i (more positive $\delta^{13}C$
464 values; Fig. 6B, S3; Table GO8). During photosynthesis, plants discriminate against $^{13}CO_2$ in the
465 reaction center of *Ribulose 1, 5-biphosphate carboxylase/oxidase* (*RuBisCO*). As stomata close to
466 minimize water loss in response to drought, the discrimination against ^{13}C is less intense because the
467 internal CO_2 concentration (C_i) becomes unavoidably reduced, reflecting a trade-off between carbon
468 gain and water loss. As a result of their reduced C_i, water-efficient plants experience lower CO_2
469 concentrations at the sites of carboxylation (C_c) and have more positive $\delta^{13}C$ values. Among the
470 candidates from our TWAS analysis that are positively related to water use efficiency, we found
471 *RuBisCO small subunit 2B* (*AT5G38420*; *RBCS2B;* Figs. 6B, D). An upregulation in *RuBisCO* may
472 compensate for suboptimal CO_2 concentrations at the sites of carboxylation that plants from drought-
473 prone environments typically experience. Among these candidates, we also find *Sedoheptulose-*

474 *bisphosphatase* (*SBPASE*, *AT3G55800*), a key enzyme in the Calvin Cycle (Lefebvre et al., 2005)
475 and *MATURATION OF RBCL 1* (*MRL1*, *AT4G34830*), a post-transcriptional regulator of *RuBisCO*
476 *large chain* (*RBCL, ATCG00490*) mRNA (Johnson et al., 2010).
477 Also among the candidates we obtained from this analysis is a member of the plasma
478 membrane intrinsic protein (PIP) subfamily of aquaporins, *PLASMA MEMBRANE INTRINSIC*
479 *PROTEIN 1;5* (*AT4G23400*; *PIP1;5*; Figs. 6B,E). While the functional role of *PIP1;5* in these
480 specific processes has not been characterized, PIPs are known to regulate water flux in guard cells as
481 well as membrane permeability to CO_2 in the mesophyll, with an important effect on mesophyll
482 conductance and CO_2 concentration at the sites of carboxylation (C_c) (Groszmann et al., 2017). Thus,
483 PIP1;5 is also a candidate regulator of photosynthetic rates. Also, among the candidates are *NADH*
484 *dehydrogenase-like complex M* (*NdhM*, *AT4G37925*), required for *NdH* complex assembly (Ifuku et
485 al., 2011), and *High cyclic electron flow 1* (*HCEF1*; *AT3G54050*) (Livingston et al., 2010), both
486 regulators of cyclic electron flow around PSI (Yamori et al., 2011), *ATP-Synthase δ-Subunit* (*ATPD*,
487 *AT4G09650*) (Maiwald et al., 2003), *Photosystem I reaction center subunit PSI-N* (*PSAN*,
488 *AT5G64040*) (Haldrup et al., 1999), *Photosystem II subunit O-2* (*PSBO2*; *AT3G50820*) (Murakami
489 et al., 2005).
490 Among the candidates that are negatively related to WUE_i, we find the transcripts of nine
491 genes, of which only two are characterized: *YELLOW STRIPE like 8* (*YSL8*, *AT1G48370*) (Waters et
492 al., 2006) and *PIGMENT DEFECTIVE EMBRYO 135* (*PDE135*, *AT2G26510*) (Niopek-Witz et al.,
493 2014). We can speculate that the large proportion of uncharacterized genes negatively associated with
494 WUE_i may be the result of an increased lethality in the loss of function mutations in these genes.
495 (Table GO9). We can further speculate that this enrichment reflects the transport of carbohydrates
496 produced during photosynthesis to promote plant growth. This would be concordant with the tradeoff
497 between growth and WUE_i that we observe in our study.
498

499 ## Limitations

500

501 Our study has revealed genetic variants associated with both plasticity and homeostasis in leaf area
502 following drought. One limitation of our study is that while the number of accessions that we utilized
503 would have been considered ample just a few years ago, with the more recent advent of GWA studies
504 in Arabidopsis such studies typically include more accessions. If the number of accessions utilized is
505 low, low-frequency variants may not be present in the subset of accessions studied. This is less of a
506 concern when we focus on variants that are undergoing selection and thus are at higher frequency in
507 the population. Accordingly, in this study, we did not consider variants in frequencies lower than
508 10% as we were interested in adaptive genetic variation. In addition, we performed TWAS, which is
509 less susceptible to this concern because it evaluates continuous variation in transcript abundance
510 rather than the presence/absence of SNPs within the study population. Indeed, RNA-seq experiments
511 often are conducted on very few genotypes, frequently comparing transcript abundance between just
512 two genotypes: wild-type and a specific mutant of interest. Another limitation typical of GWAS is
513 the fact that synthetic associations, non-causative markers that are within linkage disequilibrium with

514 causative makers, are difficult to discern from true causative markers (Korte and Farlow, 2013; Sasaki
515 et al., 2021). Identification of polygenic association signals through GWAS is also sensitive to bias
516 introduced by uncorrected population structure that can also introduce a number of false positives in
517 the resulting list of candidates (Barton et al., 2019; Sohail et al., 2019). There are statistical methods
518 to address these issues, but such methods also introduce a number of false negatives due to over-
519 correction (Korte and Farlow, 2013). Not correcting for confounding effects of population
520 stratification, family structure, and cryptic relatedness can be minimized by focusing on regional
521 collections, such as the Iberian population in this case, in which the challenges imposed by population
522 structure are reduced (Frachon et al., 2018; Tabas-Madrid et al., 2018).
523 TWAS analysis does not suffer from the limitations imposed by false non-causal synthetic
524 associations due to linkage disequilibrium and by population structure.(Korte and Farlow 2013;
525 Joehanes et al. 2017). However, TWAS analysis also presents a series of challenges, as this method
526 is sensitive to time and tissue-dependent expression (Li et al. 2020; Wainberg et al. 2019). The
527 combined analysis of reference genomic (The 1001 Genomes Consortium 2016) and transcriptomic
528 data (Kawakatsu et al. 2016), as done here, can partially ameliorate the limitations of each method.
529 The validation of candidates from both GWA and TWA studies also suffers from the
530 challenge of restricted genetic backgrounds. Most often, the characterization of knock-out mutants of
531 candidate genes is performed in a single genetic background, typically Col-0. Here, we instead
532 validated our results by meta-analysis of the larger Iberian population. TWAS in this larger sample
533 identified 31 out of the 45 candidate genes that we previously identified in the subset of 20 Iberian
534 accessions in our study for which published $\delta^{13}C$ data were available (Table T1). Moreover, there are
535 significant correlations between the results from our sample and the larger sample from both GWAS
536 and TWAS (Fig. S4).
537

538 ## Conclusion

539

540 In our study, we find a gradient ranging from higher plasticity in response to resource limitation
541 (drought) for generalist accessions originating from productive environments to increased
542 specialization and decreased phenotypic plasticity in accessions originating from more marginal
543 environments. The "passive" plasticity observed here may nevertheless be important over
544 evolutionary time as it gradually allow adaptiveness in unproductive environments as the induced
545 change in resource availability moves the mean phenotype closer to the environment-specific
546 optimum favored by selection (Waddington, 1953; Richards et al., 2006).
547 The adaptive role of plasticity has been at the center of a long-standing debate. Much work
548 and discussion have been focused on the principle that if indeed plasticity is adaptive, it may be under
549 genetic control (Bradshaw, 1965; Via et al., 1995); however, few relevant genes have been identified.
550 Here we propose that not only plasticity but also homeostasis is under genetic control and important
551 from an evolutionary standpoint. Moreover, we dissect the genetic basis of both plasticity and
552 homeostasis in leaf area, identifying specific genes and regulatory variants implicated in each process.

553 Our integrated application of GWAS, TWAS, and eGWAS identifies both candidate "plasticity
554 variants" and candidate "homeostasis variants" that can be further studied.
555 Knowledge from natural populations of how plants adapt to their environment also can be
556 incorporated in breeding and biotechnological approaches to crop improvement. We show here how
557 the integrated application of GWAS, TWAS, and eGWAS yields insights into the genetic basis of
558 responses to resource availability in Arabidopsis. A similarly integrative approach has identified
559 water use efficiency traits in sorghum (Ferguson et al., 2020). Results arising from diverse genome-
560 wide analyses in both model and crop species (Schindele et al., 2020) can now be used to inform
561 powerful new CRISPR-based approaches for gene editing and modulation of transcript abundance
562 toward crop improvement (Abudayyeh et al., 2017).
563

564 # MATERIALS AND METHODS

565

566 ## Plant materials and phenotyping

567

568 Seeds for 43 Iberian accessions (Fig. 1A and Table S1 for the list of accessions) and Col-0, which we
569 used as an internal reference, were cold-stratified for four days at 4°C to synchronize germination.
570 Plants were grown in 10 cm square pots containing Metro-mix 360 potting mixture (Sun Gro
571 Horticulture Canada Ltd) in a greenhouse with an average 500 μmol $m^{-2}s^{-1}$ photosynthetic photon
572 flux density (PPFD) and temperatures of 22 °C during the day and 20°C during the night.
573 Stratified seeds were sown in soil in the Penn State University Biology Greenhouse. We
574 imposed short day supplementary illumination (8h light: 16 h dark, with light supplied as natural
575 daylight supplemented with 1000W metal halide lamps). For each accession, we grew one plant per
576 pot, with five repetitions for each of control and drought treatments (10 plants for each individual
577 accession), for a total of 440 plants (44 accessions x five control x five droughted plants). Both control
578 and drought treatment were well-watered for the first 28 days, by maintaining the soil relative water
579 content over 75%, as measured by monitoring pot weight daily and adding water when necessary.
580 After 28 days, plants within the drought treatment were watered to soil saturation once every 10 days,
581 while the well-watered treatment was maintained near field capacity throughout the duration of the
582 experiment. The experiment continued for the entirety of the life cycle of the plants. Plants were
583 randomized within the greenhouse on a weekly basis throughout the experiment. At the end of the
584 experiment 170 days later, nine accessions within the drought treatment that encountered mortality
585 rates higher than 40% (two of the five replicates; Table S1) were excluded from downstream analysis
586 Photographs of rosettes were taken at the time of flowering and subsequently analyzed using
587 ImageJ (http://imagej.nih.gov/ij/) to determine projected leaf area. For the associations between the
588 phenotypic variables we obtained in this study, and the local environment, we inspected the data using
589 Cook's distance (Cook, 1984; Altman and Krzywinski, 2016) to evaluate the influence of each
590 datapoint on the fit. We considered values greater than 4/n to be overly influential. Based on this, we
591 decided to retain outliers in our analysis except for the phenotypic values we obtained for the
592 accession IP-Coc1 (accession id = 9535), which were consistently unrealistically influential across

593 different phenotypes based on their extreme Cook's distance. We include these removed values in
594 Table S1.
595

596 Determination of phenotypic potential and plasticity

597

598 Leaf area potential (LAP) is defined here as the normalized maximum leaf area (LA) value realized
599 by any given accession under the conditions of these experiments. This index was calculated as LAP
600 = LA_i/LA_m, where LA_i = leaf area produced by any individual accession and LA_m = average value
601 for all accessions grown under the same conditions. Accordingly, leaf area potential (LAP) reflects
602 the leaf area that any given accession displays in the absence of drought stress, divided by the average
603 leaf area of the population in the absence of drought stress. A high leaf area potential reflects a higher
604 vegetative growth of any given accession relative to the set of accessions utilized in this study. We
605 used potential rather than actual values in order to compare the relative leaf area of each accession
606 within the study population between both watering regimes.
607 Leaf area plasticity indexes were calculated based on an established definition (Bouslama and
608 Schapaugh, 1984). Leaf area plasticity indexes to drought ($LAPI_d$) were calculated as: $LAPI_d = LAP_d$
609 - LAP_{ww}; where LAP_d= leaf area potential under drought and LAP_{ww} = leaf area potential under well-
610 watered conditions. Positive indexes reflect an increment in leaf area potential value for any given
611 accession after drought treatment, not necessarily an increment in leaf area. For instance, a positive
612 leaf area plasticity index does not necessarily imply leaf areas were higher under drought, but that
613 under drought, a given accession displays a higher leaf area potential relative to the rest of accessions
614 utilized in this study.
615 Reaction norms based on leaf area potential were employed to reflect plastic changes in
616 phenotypic potential between the two treatments (well-watered vs. drought). The difference in leaf
617 area potential between drought and well-watered conditions for the reaction norm of each accession
618 is its leaf area plasticity index.
619

620 Genome-wide association study

621

622 We used a GWAS approach to identify polymorphisms associated with variation in phenotypic
623 potential and plasticity. The online tool GWAPP (http://gwas.gmi.oeaw.ac.at/) was employed using
624 a linear regression model (Seren et al., 2012). While the linear regression model does not address
625 confounding effects of population stratification, family structure and cryptic relatedness (Price et al.,
626 2010), it was employed here because those issues were minimized by our choice of a regional
627 (Iberian) population (Frachon et al., 2018; Tabas-Madrid et al., 2018; Frachon et al., 2019).
628 We filtered out low frequency variants (MAF < 10%), to focus on variants less likely to be
629 undergoing negative selection or to be spurious SNPs from sequencing errors. We obtained gene
630 model annotation from the TAIR11 genome release. We defined the 'consensus' transcript variant as
631 the variant producing the longest transcript. We predicted the effect of every SNP using SnpEff
632 (Cingolani et al., 2012)(Table G1-G6).

633 Using the results from GWAS obtained from the association with leaf area potential, we
634 obtained reaction norms that reflect plastic and homeostatic patterns of genome-wide associations of
635 these traits in response to drought. For instance, genetic association plasticity indexes to drought (G_d)
636 were calculated as: $GPI_d = G_d - G_{ww;}$ where G_d = Genome-wide association score (-log p-value) with
637 any given phenotype under drought, and G_{ww} = Genome-wide association potential under well-
638 watered conditions. The association between a phenotype and a SNP was considered more plastic as
639 the genome-wide association score difference in the correlation coefficient between the two
640 conditions reflected in the reaction norm (well-watered vs. drought) became greater. On the contrary,
641 the association between a phenotype and any given SNP was considered to be homeostatic if found
642 significantly associated to that trait under both conditions (well-watered and drought).
643

644 **Transcriptome-wide association**

645

646 We retrieved the transcriptome data generated by the Illumina HiSeq 2500 platform from rosette
647 leaves of 727 Arabidopsis accessions (without biological replicates) from the GEO dataset with
648 accession number GSE80744 and SRA study SRP074107 (Kawakatsu et al., 2016) and subsetted the
649 35 Iberian accessions that overlapped with the 43 Iberian accessions used in our study. Data
650 wrangling was conducted using the dplyr (Wickham et al., 2015) and tidyr (Wickham and Henry,
651 2018) packages. Spearman's rank correlation coefficient between individual phenotypic values and
652 individual transcript abundance values was calculated using the correlation function of the Hmisc
653 package (Harrell Jr and Dupont, 2019). The stronger the association of the two variables, the closer
654 the Pearson correlation coefficient, r, will be to either +1 or -1. We imposed a threshold based on this
655 correlation coefficient ($0.4 \geq |r| \leq 4.0$). We considered this threshold to be appropriate after inspection
656 of the results; it is a stringent value in relation to what has been used in previous TWAS studies in
657 this species ($0.3 \geq |r| \leq 3.0$) (Lan et al., 2021).
658 Using the results from TWAS obtained from the transcript abundance association with
659 phenotypic potential traits, we derived reaction norms to reflect plastic and homeostatic patterns of
660 transcriptome wide associations of these traits in response to drought. For instance, transcriptome
661 association plasticity indexes to drought ($Tr_{drought}$) were calculated as: $TrPI_{drought} = Tr_{drought} - Tr_{well-}$
662 $_{watered;}$ where $Tr_{drought}$ = transcriptome correlation coefficient potential with any given phenotype under
663 drought, and $Tr_{well-watered}$ = transcriptome correlation coefficient under well-watered conditions. The
664 association between a phenotype and any given transcript was considered to be homeostatic if found
665 significantly associated with that trait (either positively or negatively) under both conditions (well-
666 watered vs. drought). To focus on highly plastic transcriptome-wide associations, we isolated
667 association between a phenotype and transcript that met the imposed a threshold based on its
668 correlation coefficient ($0.4 \geq |r| \leq 4.0$) under one condition (well-watered or drought), but with a
669 reaction norm that crossed the lack of correlation value ($r = 0$).
670

671 **eGWAS**

672

673 eGWAS was conducted by compiling the transcript abundance values of any given gene and
674 extracting transcript abundance for that particular gene in the 727 Arabidopsis accessions from the
675 GEO dataset with accession number GSE80744 and SRA study SRP074107 (Kawakatsu et al., 2016),
676 then subsetting the 665 accessions included in the 1001 Genomes project (The 1001 Genomes
677 Consortium, 2016). Regulatory variants are either cis or trans acting, depending on the physical
678 distance between the genetic variant. cis-eSNPs were defined as those located within the ORF or the
679 promoter region, which was defined as 5 kb upstream of the most distal transcription start site of the
680 gene. Trans-eSNPs were defined as those located within the ORF/promoter region of a gene different
681 from the one that is transcriptionally regulated by that genetic variant.

682 **Meta-analysis of Iberian Arabidopsis accessions**

683

684 To explore the local environment of this population, we retrieved 204 environmental parameters for
685 these 188 Iberian accessions from AraCLIM (https://github.com/CLIMtools/AraCLIM) (Table
686 SXX1). AraCLIM is a database that describes the local environment of the Arabidopsis accessions
687 sequenced as part of the 1001 Genomes Project (Ferrero-Serrano and Assmann, 2019). We obtained
688 from AraCLIM the moderate-resolution imaging spectroradiometer data corresponding to the spring
689 months during the 2001-2010 period, to assess the Net Primary Productivity in the local environment
690 of the accessions included in our study. (MOD17A2; Net Primary Productivity in the spring season)
691 (Heinsch et al., 2003; Running and Zhao, 2015)
692 To integrate the information from previously published studies that included accessions from
693 the Iberian Arabidopsis population, we retrieved available data on natural variation in intrinsic water
694 use efficiency (WUEi, $\delta^{13}C$) previously recorded by Dittberner et al. (2018) from PhenoCLIM
695 (https://github.com/CLIMtools/PhenoCLIM)(Table P1,P2)(Ferrero-Serrano and Assmann, 2019).

696 **Analyses**

697

698 All statistical analyses and figures were produced using R (Team, 2013). The code and data to easily
699 reproduce the analysis, figures and tables in this manuscript are available at
700 https://github.com/AssmannLab and Zenodo. Gene Ontology (GO) biological process analysis was
701 performed using the open-source software ShinyGO v0.61: http://bioinformatics.sdstate.edu/go60/
702 (Ge et al., 2020) with the following settings: the search species was "*Arabidopsis thaliana*," the *P*-
703 value cutoff (FDR) was 0.05, and the number of most significant terms to show was 10. To replicate
704 these results, the lists of genes that were input into these analyses based on significance thresholds
705 can be selected from Table G1-G6, T1,T2.
706

707 **Supplemental data**

708

709 The following supplemental materials are available

Figure S1. Genotypic and transcriptomic reaction norms based the strength of association of individual SNPs and transcripts highlights the variation of these associations depending on water availability.

Figure S2. Accessions from more productive areas display stronger negative plastic reductions in leaf area relative to accessions from less productive environments

Figure S3. Illustration of the photosynthesis-related transcript variants that regulate water use efficiency in Iberian Arabidopsis accession**.**

Figure S4. The accessions included in this study are representative of the Iberian accessions included in the 1001 Genomes project.

Table P1. Leaf area measurements recorded in this experiment (well-watered & drought). Calculated leaf area potential and plasticity, water use efficiency (WUE_i, $\delta^{13}C$) values recorded by Dittberner et al. (2018) and MOD17A2 net primary productivity) information obtained from AraCLIM (Ferrero-Serrano & Assmann, 2019) for the accessions included in our study.

Table P2. Water use efficiency (WUEi, $\delta^{13}C$) values recorded by Dittberner et al. (2018) for 95 Iberian Arabidopsis accessions.

Table G1. Candidates obtained from GWAS on leaf area potential under well-watered conditions. Only associations with a score ≥ 4 are included here. For a pre-filtered, as well as a full filtered version of this file, please visit the data repository.

Table G2. Candidates obtained from GWAS on leaf area potential under drought. Only associations with a score ≥ 4 are included here. For a full pre-annotated and filtered, as well as a full annotated and filtered version of this file, please visit the data repository. For a pre-filtered, as well as a full filtered version of this file, please visit the data repository.

Table G3. Candidates obtained from GWAS on leaf area plasticity. Only associations with a score ≥ 4 are included here. For a pre-filtered, as well as a full filtered version of this file, please visit the data repository.

Table G4. Candidates obtained from GWAS on water use efficiency (WUEi, δ13C) values recorded by Dittberner et al. (2018) for the accessions included in our study. Only associations with a score ≥ 4 are included here. For a pre-filtered, as well as a full filtered version of this file, please visit the data repository.

Table G5. Candidates obtained from GWAS on water use efficiency (WUEi, δ13C) values recorded by Dittberner et al. (2018) for 95 Iberian Arabidopsis accessions. For a pre-filtered, as well as a full filtered version of this file, please visit the data repository.

Table G6. Candidates obtained from eGWAS on the natural variation in transcript abundance of SAUR26 extracted from Kawakatsu et al. (2016). For a pre-filtered, as well as a full filtered version of this file, please visit the data repository.

Table T1. Results from TWAS (r_s).

Table T2. Results from TWAS (*P*-value).

749 **Table GO1.** GO analysis on the 17 genes corresponding to the top 50 candidate SNPs resulting from
750 GWAS analysis on leaf area potential under well-watered conditions.
751 **Table GO2.** GO analysis on negatively correlated candidates resulting from TWAS analysis on leaf
752 area potential under well-watered conditions.
753 **Table GO3.** GO analysis on the 30 genes corresponding to the top 50 candidate SNPs resulting from
754 GWAS analysis on leaf area plasticity index for drought.
755 **Table GO4.** GO analysis on the positively correlated candidates resulting from TWAS analysis on
756 leaf area plasticity index for drought.
757 **Table GO5.** GO analysis on the negatively correlated candidates resulting from TWAS analysis on
758 leaf area plasticity index for drought.
759 **Table GO5.** GO analysis on the transcripts with abundances that overlap negatively with leaf area
760 potential under well-watered conditions, and positively with leaf area plasticity index for drought
761 (blue datapoints in Fig. 4C).
762 **Table GO6.** GO analysis on the transcripts with abundances that overlap negatively with leaf area
763 potential under well-watered conditions, and positively with leaf area plasticity index for drought
764 (orange datapoints in Fig. 4C).
765 **Table GO7.** GO analysis on the transcripts with abundances that overlap negatively with leaf area
766 plasticity index for drought and WUEi (red datapoints in Fig. 4F).
767 **Table GO8**. GO analysis on the positively correlated candidates resulting from TWA analysis of
768 water use efficiency determined from (δ13C) values in 88 Iberian Arabidopsis accessions (Fig. 6A).
769 **Table GO9.** GO analysis on the negatively correlated candidates resulting from TWA analysis of
770 water use efficiency determined from (δ13C) values in 88 Iberian Arabidopsis accessions (Fig. 6A).
771

772 # Figures

773 **Figure 1. Rosette leaf area observations at the time of flowering used to calculate leaf area**
774 **potential and plasticity in this study (Table S1). A**. Detail of the common garden experiment,
775 illustrating the randomization of well-watered and drought treatments, as reflected in soil coloration.
776 **B.** Leaf areas for accessions grown under optimal conditions. **C**. Leaf areas for accessions under
777 drought conditions. Accessions are arranged alphabetically. Bars represent means ±SE. **D.** Images
778 illustrating the plastic and homeostatic responses to drought found among the accessions included in
779 this study. **E.** Phenotypic reaction norms illustrating an overall reduction of leaf area in response to
780 drought (t-test; P-value < 0.001). Violin distributions represent probability densities of leaf area (cm^2)
781 among the accessions included in this study. Datapoints depict the mean phenotypic values of
782 individual accessions, and the reaction norms represent the plastic response in the leaf area of each
783 accession in response to drought. **F** Phenotypic reaction norms illustrating plastic and homeostatic
784 responses in leaf area potential (t-test; P-value > 0.05). Violin distributions represent probability
785 densities of leaf area potential among the accessions included in this study. Datapoints depict the leaf
786 area potential of individual accessions, and the reaction norms represent the plastic response in the

787 leaf area of leaf area potential of each accession in response to drought.

788 **Figure 2. *SMALL AUXIN UP RNA 26* (*SAUR26,* AT3G03850) is a candidate regulator of leaf**
789 **plasticity in response to drought. A.** Manhattan plot representing the strength of association
790 between genetic variants and leaf area plasticity in response to drought and illustration of the GO
791 analysis enrichment found for the 50 variants displaying the strongest strength of association with
792 this plasticity index. **B.** *SAUR26* gene model, including the two co-varying SNPs highlighted in **3B**.
793 Orange block depicts the single exon, green block the 5' UTR, dark green the 3' UTR. Labels above
794 indicate the position of the two SNPs that co-vary forming a haplotype in our sample. The illustration
795 includes information on the major/minor allele corresponding to each of the SNPs, its frequency in
796 our sample, in 189 accessions from the Iberian within the 1001 Genome Project, and in the whole
797 1001 Genome Project sample dataset. **C.** Manhattan plot representing the genome-wide strength of
798 association between the genetic variation present within the 665 accessions from the transcript
799 abundance reference panel used in this study (Kawakatsu et al., 2016) that overlap with the collection
800 of accessions included in the 1001 Genomes project, and the variation in the transcript abundance of
801 *SAUR26* (Kawakatsu et al., 2016). The peak in chromosome 3 represents the cis-genetic variants in
802 *SAUR26* affecting its transcript abundance. For **B** and **C**, the score (y-axis) consists of the negative
803 logarithm of the *P*-value and provides association strength. Each data point represents an SNP with
804 a color corresponding to the chromosome where the genetic variants are located. The x-axis and the
805 different colors shown in the SNPs depicted in the Manhattan plots represent the different
806 chromosomes. The higher the score, the lower the P-value, and the stronger the association between
807 genetic variation and leaf area plasticity or *SAUR26* transcript abundance. **D.** The minor haplotype of
808 *SAUR26* is associated with negative plastic responses of leaf area potential in response to drought.
809 Conversely, the major haplotype is associated with homeostatic or positive responses in leaf area
810 potential in response to drought. Violin plots showing significantly different probability densities of
811 leaf area plasticity in response to drought for the major and minor allele haplotypes in *SAUR26.* **E.**
812 The haplotype in *SAUR26* associated with leaf area plasticity/homeostasis in response to drought is
813 a regulatory haplotype. Violin plots showing significantly different probability densities of *SAUR26*
814 transcript abundance for the major and minor allele haplotypes in *SAUR26* for both our sample and
815 the entire Iberian population. **F.** Scatter plot illustrating the positive relationship between leaf area
816 plasticity index (y-axis) and *SAUR26* transcript abundance (x-axis). Grey shadow represents the 95%
817 CI of the fit regression line (dark grey). **G**. Cartoon illustrating the regulatory role of genetic and
818 transcript variation in *SAUR26* and the response of leaf area to drought.

819 **Figure 3. Transcriptomic reaction norms uncover the genetic correlates of leaf area homeostasis**
820 **in response to drought. A.** Transcriptomic homeostatic reaction norms for leaf area in response to
821 drought. This plot depicts the homeostatic relationship between the association of transcript
822 abundance for each gene and leaf area potential under well-watered vs. drought conditions.
823 Spearman's rank correlation coefficient ($r_{s;}$ y-axis) indicates the correlation between the leaf area
824 potential and the natural variation in transcript abundance of each gene. The upper panel shows
825 homeostatic reaction norms for transcripts significantly and positively correlated with leaf area

826 potential under both watering regimes. The bottom panel shows homeostatic reaction norms for
827 transcripts significantly and negatively correlated with leaf area potential under both watering
828 regimes. **B** and **C**. Scatter plots depicting the relationship (*P*-value < 0.05) between leaf area potential
829 under both well-watered and drought conditions (y-axis), and transcript abundance (FPKM; x-axis)
830 of *ILI1 binding bHLH 1* (*IBH1,* AT2G43060) (**B)** and *RING-H2 GROUP F1A* (*RHF1A*; *AT4G14220*)
831 **(C)**. In both (C) and (D), data were fitted using a linear regression model. Dark circles depict the leaf
832 area potential of accessions grown under well-watered conditions, while gray squares depict the leaf
833 area potential of accessions grown under drought.
834

835 **Figure 4. Accessions with lower leaf area potential display leaf area homeostasis and higher**
836 **water use efficiency as defined by $\delta^{13}C$. A.** Negative relationship (*P*-value < 0.05) between leaf area
837 plasticity in response to drought (y-axis) and leaf area potential under well-watered conditions (x-
838 axis). Data were fitted using a linear regression model. Grey shadow represents the 95% CI of the fit
839 regression line. Four different quadrants are defined by two dashed lines: the average leaf area
840 potential (x-axis), and y = 0, which is the homeostatic point at which a change in water availability
841 does not affect phenotypic potential. Data points depict individual accessions with their respective
842 label. Data points are colored based on in which quadrant they fall (see text). **B**. The genetic basis of
843 leaf area potential and plasticity in response to drought. Relationship between the GWAS associations
844 found for the plastic responses in leaf area after drought (x-axis) (Table G3) and leaf area potential
845 in the absence of drought (y-axis) (Table G1). Data points represent individual SNPs. Dashed lines
846 depict an arbitrary threshold of 4 for significance. **C.** Transcriptomic association with leaf area
847 potential under well-watered conditions and plastic leaf area responses to drought. Spearman's rank
848 correlation depicts the relationship between the association for the transcript abundance of each gene
849 in the Arabidopsis genome with leaf area plasticity in response to drought (r_s) in the y-axis and leaf
850 area potential in the x-axis. Dashed lines define an arbitrary threshold to consider transcripts
851 correlated positively ($r_s \geq 0.4$) or negatively ($r_s \leq -0.4$) with leaf area plasticity (y-axis) or net primary
852 productivity (x-axis). **D.** Scatter plot illustrating the positive relationship (*P*-value < 0.05) between
853 leaf area homeostasis in response to drought (leaf area plasticity index, y-axis) and water use
854 efficiency (x-axis) among Iberian Arabidopsis accessions used in this study. Data were fitted to a
855 linear regression model. Grey shadow represents the 95% CI of the fit regression line (black). $\delta^{13}C$
856 data for the accessions studied here were retrieved from (Dittberner et al., 2018). As in panel **A**, four
857 different quadrants are defined by two dashed lines: y = 0, which is the homeostatic point at which a
858 change in water availability does not affect leaf area potential (i.e., a plasticity index of 0), and the
859 average intrinsic water use efficiency (WUE_i, $\delta^{13}C$; x-axis). Data points depict individual accessions
860 with their respective labels. **E.** The genetic basis of leaf area plasticity in response to drought and
861 water use efficiency. This plot depicts the respective relationship between the GWAS associations
862 found for the leaf area plasticity index in response to drought (y-axis) and water use efficiency
863 (Dittberner et al., 2018) (x-axis). Data points represent individual SNPs. The y-axis and x-axis depict
864 the extent of the association with, respectively, leaf area plasticity, and WUE_i, as the negative
865 logarithm of the p-value. Dashed lines depict an arbitrary threshold for significance that is consistent

across comparisons. **F.** Transcriptomic association with plastic leaf area responses to drought and WUE_i. Spearman's rank correlation depicts the relationship between the association for the transcript abundance of each gene in the Arabidopsis genome with leaf area plasticity in response to drought (r_s) in the y-axis and with WUE_i in the x-axis. Dashed lines define an arbitrary threshold to consider transcripts correlated positively ($r_s \geq 0.4$) or negatively ($r_s \leq -0.4$) with leaf area plasticity (y-axis) or net primary productivity (x-axis).

Figure 5. *CNGC16* and *AHA4* exemplify transcripts with opposing relationships to leaf area plasticity and water use efficiency. A and **B**. Scatter plots depicting the relationship (*P*-value < 0.05) between (**A**) leaf area plasticity index in response to drought or (**B**) water use efficiency (Dittberner et al., 2018) in the y-axis, and transcript abundance (FPKM) of *CYCLIC NUCLEOTIDE-GATED CHANNEL 16* (*CNGC16*) in the x-axis. **C** and **D**. Scatter plots depicting the relationship (P-value < 0.05) between leaf area plasticity index in response to drought (**5C**), or water use efficiency (**5D**) in the y-axis, and transcript abundance (FPKM) of *H^+-ATPase 4* (*AHA4*) in the x-axis. In all panels, data were fitted using a linear regression model. Grey shadow represents the 95% CI of the fit regression line.

Figure 6. Photosynthesis-related transcript variants regulate water use efficiency in Iberian Arabidopsis accessions. A. Manhattan plot representing the genome-wide strength of association between genetic variation and natural variation in $\delta^{13}C$ present within the 95 Iberian accessions of our study, with $\delta^{13}C$ values retrieved from (Dittberner et al., 2018). The score (y-axis) consists of the negative logarithm of the *P*-value and provides association strength. **Inset:** Violin plots representing the probability densities of water use efficiency for the major and minor allele haplotypes in *ClpX* for the accessions included in 6A**. B.** T-Manhattan plot representing transcriptome-wide strength of association between variation in transcript abundance (Kawakatsu et al., 2016) and natural variation in $\delta^{13}C$. In this analysis, we included the Iberian accessions with both transcript abundance data (Kawakatsu et al., 2016) and $\delta^{13}C$ information (Dittberner et al., 2018). The relationship is defined by the Spearman's rank correlation coefficient (r_s). Dashed lines define an arbitrary threshold for positive ($r_s \geq 0.4$) or negative ($r_s \leq -0.4$) correlation with water-use efficiency (y-axis). **C**. Scatter plot depicting the positive relationship (*P*-value < 0.05) between WUE_i (y-axis) and *PLASMA MEMBRANE INTRINSIC PROTEIN 1;5* (*PIP1;5, AT4G23400*) transcript abundance for the Iberian accessions included in 6B. **D**. Scatter plot depicting the positive relationship (*P*-value < 0.05) between WUE_i (y-axis) and *RuBisCO SMALL SUBUNIT 2B* (*AT5G38420*; *RBCS2B*) transcript abundance for the Iberian accessions included in 6B. **E**. Scatter plot depicting the positive relationship (*P*-value < 0.05) between intrinsic water-use efficiency (WUE_i; y-axis) and *SMALL AUXIN UP RNA 26* (*SAUR26,* AT3G03850) transcript abundance for the Iberian accessions included in 6B. For **C**, **D**, and **E**, gray shadow represents the 95% CI of the fit regression line (black).

Acknowledgements

This research was supported by funding from The Pennsylvania State University to S.M.A.

References

Abudayyeh OO, Gootenberg JS, Essletzbichler P, Han S, Joung J, Belanto JJ, Verdine V, Cox DBT, Kellner MJ, Regev A, et al (2017) RNA targeting with CRISPR-Cas13. Nature 550: 280–284

Altman N, Krzywinski M (2016) Analyzing outliers: influential or nuisance? Nat Methods 13: 281–282

Angert AL, Huxman TE, Chesson P, Venable DL (2009) Functional tradeoffs determine species coexistence via the storage effect. Proc Natl Acad Sci USA 106: 11641–11645

Baek D, Kim MC, Kumar D, Park B, Cheong MS, Choi W, Park HC, Chun HJ, Park HJ, Lee SY, et al (2019) *AtPR5K2*, a *PR5-Like Receptor Kinase*, Modulates Plant Responses to drought Stress by *phosphorylating protein phosphatase 2Cs*. Front Plant Sci 10: 1146

Barton N, Hermisson J, Nordborg M (2019) Population genetics: Why structure matters. Elife 8: e45380

Billings WD, Mooney HA (1968) The ecology of arctic and alpine plants. Biol Rev 43: 481–529

Bouslama M, Schapaugh WT (1984) Stress tolerance in soybeans. I. evaluation of three screening techniques for heat and drought tolerance. Crop Sci 24: 933–937

Bradshaw AD (1965) Evolutionary significance of phenotypic plasticity in plants. Elsevier, pp 115–155

Cao J, Schneeberger K, Ossowski S, Günther T, Bender S, Fitz J, Koenig D, Lanz C, Stegle O, Lippert C, et al (2011) Whole-genome sequencing of multiple *Arabidopsis thaliana* populations. Nat Genet 43: 956–963

Chapin, FS (1991) Integrated responses of plants to stress. Bioscience 41: 29–36

Chen I-C, Hill JK, Ohlemüller R, Roy DB, Thomas CD (2011) Rapid range shifts of species associated with high levels of climate warming. Science 333: 1024–1026

Cingolani P, Platts A, Wang LL, Coon M, Nguyen T, Wang L, Land SJ, Lu X, Ruden DM (2012) A program for annotating and predicting the effects of single nucleotide polymorphisms, SnpEff: SNPs in the genome of *Drosophila melanogaster* strain w1118; iso-2; iso-3. Fly (Austin) 6: 80–92

Coll JR, Aguilar E, Ashcroft L (2016) Drought variability and change across the Iberian Peninsula. Theoretical and Applied Climatology 1–16

Condon AG, Richards RA, Rebetzke GJ, Farquhar GD (2002) Improving intrinsic water-use efficiency and crop yield. Crop Sci 42: 122–131

Cook RD (1984) Assessment of local influence. doi: 10.21236/ADA143002

De Veylder L, Beeckman T, Beemster GT, Krols L, Terras F, Landrieu I, van der Schueren E, Maes S, Naudts M, Inzé D (2001) Functional analysis of cyclin-dependent kinase inhibitors of Arabidopsis. Plant Cell 13: 1653–1668

942 DeFalco TA, Moeder W, Yoshioka K (2016) Opening the gates: insights into cyclic nucleotide-
943 gated channel-mediated signaling. Trends Plant Sci 21: 903–906
944 Des Marais DL, McKay JK, Richards JH, Sen S, Wayne T, Juenger TE (2012) Physiological
945 genomics of response to soil drying in diverse Arabidopsis accessions. Plant Cell 24: 893–
946 914
947 Dittberner H, Korte A, Mettler-Altmann T, Weber APM, Monroe G, de Meaux J (2018) Natural
948 variation in stomata size contributes to the local adaptation of water-use efficiency in
949 *Arabidopsis thaliana*. Mol Ecol 27: 4052–4065
950 Donat MG, Lowry AL, Alexander LV, O'Gorman PA, Maher N (2016) More extreme precipitation
951 in the world's dry and wet regions. Nat Clim Chang 6: 508–513
952 Dorn LA, Pyle EH, Schmitt J (2000) Plasticity to light cues and resources in *Arabidopsis thaliana*:
953 testing for adaptive value and costs. Evolution 54: 1982–1994
954 Du S-S, Li L, Li L, Wei X, Xu F, Xu P, Wang W, Xu P, Cao X, Miao L, et al (2020) Photoexcited
955 *Cryptochrome2* interacts directly with *TOE1* and *TOE2* in flowering regulation. Plant
956 Physiol 184: 487–505
957 Durvasula A, Fulgione A, Gutaker RM, Alacakaptan SI, Flood PJ, Neto C, Tsuchimatsu T, Burbano
958 HA, Picó FX, Alonso-Blanco C, et al (2017) African genomes illuminate the early history
959 and transition to selfing in *Arabidopsis thaliana*. Proc Natl Acad Sci USA 114: 5213–5218
960 Easlon HM, Nemali KS, Richards JH, Hanson DT, Juenger TE, McKay JK (2014) The
961 physiological basis for genetic variation in water use efficiency and carbon isotope
962 composition in *Arabidopsis thaliana*. Photosyn Res 119: 119–129
963 Easterling DR, Meehl GA, Parmesan C, Changnon SA, Karl TR, Mearns LO (2000) Climate
964 extremes: observations, modeling, and impacts. Science 289: 2068–2074
965 Exposito-Alonso M, 500 Genomes Field Experiment Team, Burbano HA, Bossdorf O, Nielsen R,
966 Weigel D (2019) Natural selection on the *Arabidopsis thaliana* genome in present and
967 future climates. Nature 573: 126–129
968 Exposito-Alonso M, Brennan AC, Alonso-Blanco C, Picó FX (2018a) Spatio-temporal variation in
969 fitness responses to contrasting environments in *Arabidopsis thaliana*. Evolution. doi:
970 10.1111/evo.13508
971 Exposito-Alonso M, Vasseur F, Ding W, Wang G, Burbano HA, Weigel D (2018b) Genomic basis
972 and evolutionary potential for extreme drought adaptation in *Arabidopsis thaliana*. Nat Ecol
973 Evol 2: 352–358
974 Ferguson JN, Fernandes SB, Monier B, Miller ND, Allan D, Dmitrieva A, Schmuker P, Lozano R,
975 Valluru R, Buckler ES, et al (2020) Machine learning enabled phenotyping for GWAS and
976 TWAS of WUE traits in 869 field-grown sorghum accessions. BioRxiv. doi:
977 10.1101/2020.11.02.365213
978 Ferrero-Serrano Á, Assmann SM (2019) Phenotypic and genome-wide association with the local
979 environment of Arabidopsis. Nat Ecol Evol 3: 274–285
980 Ferrero-Serrano Á, Assmann SM (2016) The α-subunit of the rice heterotrimeric G protein, RGA1,
981 regulates drought tolerance during the vegetative phase in the dwarf rice mutant *d1*. J Exp

982 Bot 67: 3433–3443
983 Ferrero-Serrano Á, Su Z, Assmann SM (2018) Illuminating the role of the Gα heterotrimeric G
984 protein subunit, *RGA1*, in regulating photoprotection and photoavoidance in rice. Plant Cell
985 Environ 41: 451–468
986 Fisher RA (1919) The correlation between relatives on the supposition of mendelian inheritance.
987 Trans R Soc Edinb 52: 399–433
988 Forsman A (2015) Rethinking phenotypic plasticity and its consequences for individuals,
989 populations and species. Heredity 115: 276–284
990 Frachon L, Bartoli C, Carrère S, Bouchez O, Chaubet A, Gautier M, Roby D, Roux F (2018) A
991 genomic map of climate adaptation in *Arabidopsis thaliana* at a micro-geographic scale.
992 Front Plant Sci 9: 967
993 Frachon L, Mayjonade B, Bartoli C, Hautekèete N-C, Roux F (2019) Adaptation to plant
994 communities across the genome of *Arabidopsis thaliana*. Mol Biol Evol 36: 1442–1456
995 Galton F (1894) Natural inheritance. Macmillan and Company
996 Gao Q-M, Venugopal S, Navarre D, Kachroo A (2011) Low oleic acid-derived repression of
997 jasmonic acid-inducible defense responses requires the *WRKY50* and *WRKY51* proteins.
998 Plant Physiol 155: 464–476
999 Ge SX, Jung D, Yao R (2020) ShinyGO: a graphical gene-set enrichment tool for animals and
1000 plants. Bioinformatics 36: 2628–2629
1001 Ghalambor CK, McKAY JK, Carroll SP, Reznick DN (2007) Adaptive versus non-adaptive
1002 phenotypic plasticity and the potential for contemporary adaptation in new environments.
1003 Funct Ecol 21: 394–407
1004 Gomaa NH, Montesinos-Navarro A, Alonso-Blanco C, Picó FX (2011) Temporal variation in
1005 genetic diversity and effective population size of Mediterranean and subalpine *Arabidopsis*
1006 *thaliana* populations. Mol Ecol 20: 3540–3554
1007 Grime JP (1977) Evidence for the existence of three primary strategies in plants and its relevance to
1008 ecological and evolutionary theory. Am Nat 111: 1169–1194
1009 Groszmann M, Osborn HL, Evans JR (2017) Carbon dioxide and water transport through plant
1010 aquaporins. Plant Cell Environ 40: 938–961
1011 Gusev A, Ko A, Shi H, Bhatia G, Chung W, Penninx BWJH, Jansen R, de Geus EJC, Boomsma DI,
1012 Wright FA, et al (2016) Integrative approaches for large-scale transcriptome-wide
1013 association studies. Nat Genet 48: 245–252
1014 Hager A (2003) Role of the plasma membrane H+-ATPase in auxin-induced elongation growth:
1015 historical and new aspects. J Plant Res 116: 483–505
1016 Haldrup A, Naver H, Scheller HV (1999) The interaction between plastocyanin and photosystem I
1017 is inefficient in transgenic Arabidopsis plants lacking the *PSI-N* subunit of photosystem I.
1018 Plant J 17: 689–698
1019 Harrell Jr F, Dupont C (2019) Package 'Hmisc'. CRAN2018 2019: 235–6
1020 Heinsch FA, Reeves M, Votava P, Kang S, Milesi C, Zhao M, Glassy J, Jolly WM, Loehman R,
1021 Bowker CF, et al (2003) Gpp and npp (mod17a2/a3) products nasa modis land algorithm.

1022 MOD17 User's Guide 1–57
1023 Holt RD (1990) The microevolutionary consequences of climate change. Trends Ecol Evol (Amst)
1024 5: 311–315
1025 Ifuku K, Endo T, Shikanai T, Aro E-M (2011) Structure of the chloroplast NADH dehydrogenase-
1026 like complex: nomenclature for nuclear-encoded subunits. Plant Cell Physiol 52: 1560–1568
1027 Ikeda M, Fujiwara S, Mitsuda N, Ohme-Takagi M (2012) A triantagonistic basic helix-loop-helix
1028 system regulates cell elongation in Arabidopsis. Plant Cell 24: 4483–4497
1029 Johnson X, Wostrikoff K, Finazzi G, Kuras R, Schwarz C, Bujaldon S, Nickelsen J, Stern DB,
1030 Wollman F-A, Vallon O (2010) *MRL1*, a conserved Pentatricopeptide repeat protein, is
1031 required for stabilization of *rbcL* mRNA in Chlamydomonas and Arabidopsis. Plant Cell 22:
1032 234–248
1033 Juenger TE, McKay JK, Simms EI, Richards JH (2005) Identification and characterization of QTL
1034 underlying whole-plant physiology in *Arabidopsis thaliana*: $\delta^{13}C$, stomatal conductance and
1035 transpiration efficiency. Plant Cell Environ 28: 697–708
1036 Kasuga M, Liu Q, Miura S, Yamaguchi-Shinozaki K, Shinozaki K (1999) Improving plant drought,
1037 salt, and freezing tolerance by gene transfer of a single stress-inducible transcription factor.
1038 Nat Biotechnol 17: 287–291
1039 Kawakatsu T, Huang S-SC, Jupe F, Sasaki E, Schmitz RJ, Urich MA, Castanon R, Nery JR,
1040 Barragan C, He Y, et al (2016) Epigenomic diversity in a global collection of *Arabidopsis*
1041 *thaliana* accessions. Cell 166: 492–505
1042 Kim J, Rudella A, Ramirez Rodriguez V, Zybailov B, Olinares PDB, van Wijk KJ (2009) Subunits
1043 of the plastid ClpPR protease complex have differential contributions to embryogenesis,
1044 plastid biogenesis, and plant development in Arabidopsis. Plant Cell 21: 1669–1692
1045 Kimball S, Gremer JR, Angert AL, Huxman TE, Venable DL (2012) Fitness and physiology in a
1046 variable environment. Oecologia 169: 319–329
1047 van Kleunen M, Fischer M (2005) Constraints on the evolution of adaptive phenotypic plasticity in
1048 plants. New Phytol 166: 49–60
1049 Köhler C, Merkle T, Neuhaus G (1999) Characterisation of a novel gene family of putative cyclic
1050 nucleotide- and calmodulin-regulated ion channels in *Arabidopsis thaliana*. Plant J 18: 97–
1051 104
1052 Korte A, Farlow A (2013) The advantages and limitations of trait analysis with GWAS: a review.
1053 Plant Methods 9: 29
1054 Kremling KAG, Diepenbrock CH, Gore MA, Buckler ES, Bandillo NB (2019) Transcriptome-wide
1055 association supplements genome-wide association in *Zea mays*. G3 (Bethesda) 9: 3023–
1056 3033
1057 Lan Y, Sun R, Ouyang J, Ding W, Kim M-J, Wu J, Li Y, Shi T (2021) AtMAD: *Arabidopsis*
1058 *thaliana* multi-omics association database. Nucleic Acids Res 49: D1445–D1451
1059 Lasky JR, Des Marais DL, Lowry DB, Povolotskaya I, McKay JK, Richards JH, Keitt TH, Juenger
1060 TE (2014) Natural variation in abiotic stress responsive gene expression and local
1061 adaptation to climate in *Arabidopsis thaliana*. Mol Biol Evol 31: 2283–2296

1062 Lefebvre S, Lawson T, Zakhleniuk OV, Lloyd JC, Raines CA, Fryer M (2005) Increased
1063 sedoheptulose-1,7-bisphosphatase activity in transgenic tobacco plants stimulates
1064 photosynthesis and growth from an early stage in development. Plant Physiol 138: 451–460
1065 Leyser HM, Pickett FB, Dharmasiri S, Estelle M (1996) Mutations in the *AXR3* gene of Arabidopsis
1066 result in altered auxin response including ectopic expression from the *SAUR-AC1* promoter.
1067 Plant J 10: 403–413
1068 Li Z-G, Chen H-W, Li Q-T, Tao J-J, Bian X-H, Ma B, Zhang W-K, Chen S-Y, Zhang J-S (2015)
1069 Three SAUR proteins *SAUR76*, *SAUR77* and *SAUR78* promote plant growth in Arabidopsis.
1070 Sci Rep 5: 12477
1071 Liu J, Zhang Y, Qin G, Tsuge T, Sakaguchi N, Luo G, Sun K, Shi D, Aki S, Zheng N, et al (2008)
1072 Targeted degradation of the cyclin-dependent kinase inhibitor ICK4/KRP6 by RING-type
1073 E3 ligases is essential for mitotic cell cycle progression during Arabidopsis gametogenesis.
1074 Plant Cell 20: 1538–1554
1075 Livingston AK, Cruz JA, Kohzuma K, Dhingra A, Kramer DM (2010) An Arabidopsis mutant with
1076 high cyclic electron flow around photosystem I (hcef) involving the NADPH dehydrogenase
1077 complex. Plant Cell 22: 221–233
1078 Lobo JM, Castro I, Moreno JC (2001) Spatial and environmental determinants of vascular plant
1079 species richness distribution in the Iberian Peninsula and Balearic Islands. Biological
1080 Journal of the Linnean Society 73: 233–253
1081 Loik ME, Breshears DD, Lauenroth WK, Belnap J (2004) A multi-scale perspective of water pulses
1082 in dryland ecosystems: climatology and ecohydrology of the western USA. Oecologia 141:
1083 269–281
1084 Maiwald D, Dietzmann A, Jahns P, Pesaresi P, Joliot P, Joliot A, Levin JZ, Salamini F, Leister D
1085 (2003) Knock-out of the genes coding for the Rieske protein and the ATP-synthase delta-
1086 subunit of Arabidopsis. Effects on photosynthesis, thylakoid protein composition, and
1087 nuclear chloroplast gene expression. Plant Physiol 133: 191–202
1088 Manzano-Piedras E, Marcer A, Alonso-Blanco C, Picó FX (2014) Deciphering the adjustment
1089 between environment and life history in annuals: lessons from a geographically-explicit
1090 approach in *Arabidopsis thaliana*. PLoS One 9: e87836
1091 Marcer A, Vidigal DS, James PMA, Fortin MJ, Méndez-Vigo B, Hilhorst HWM, Bentsink L,
1092 Alonso-Blanco C, Picó FX (2018) Temperature fine-tunes Mediterranean *Arabidopsis*
1093 *thaliana* life-cycle phenology geographically. Plant Biol (Stuttg) 20 Suppl 1: 148–156
1094 Meehl GA, Tebaldi C (2004) More intense, more frequent, and longer lasting heat waves in the 21st
1095 century. Science 305: 994–997
1096 Méndez-Vigo B, Picó FX, Ramiro M, Martínez-Zapater JM, Alonso-Blanco C (2011) Altitudinal
1097 and climatic adaptation is mediated by flowering traits and FRI, FLC, and PHYC genes in
1098 Arabidopsis. Plant Physiol 157: 1942–1955
1099 Montesinos A, Tonsor SJ, Alonso-Blanco C, Picó FX (2009) Demographic and genetic patterns of
1100 variation among populations of *Arabidopsis thaliana* from contrasting native environments.
1101 PLoS One 4: e7213

1102 Montesinos-Navarro A, Wig J, Pico FX, Tonsor SJ (2011) *Arabidopsis thaliana* populations show
1103 clinal variation in a climatic gradient associated with altitude. New Phytol 189: 282–294
1104 Moreno JE, Moreno-Piovano G, Chan RL (2018) The antagonistic basic helix-loop-helix partners
1105 BEE and IBH1 contribute to control plant tolerance to abiotic stress. Plant Sci 271: 143–150
1106 Murakami R, Ifuku K, Takabayashi A, Shikanai T, Endo T, Sato F (2005) Functional dissection of
1107 two Arabidopsis PsbO proteins: *PsbO1* and *PsbO2*. FEBS J 272: 2165–2175
1108 Nagatoshi Y, Ikeda M, Kishi H, Hiratsu K, Muraguchi A, Ohme-Takagi M (2016) Induction of a
1109 dwarf phenotype with IBH1 may enable increased production of plant-made
1110 pharmaceuticals in plant factory conditions. Plant Biotechnol J 14: 887–894
1111 Niopek-Witz S, Deppe J, Lemieux MJ, Möhlmann T (2014) Biochemical characterization and
1112 structure-function relationship of two plant NCS2 proteins, the nucleobase transporters
1113 *NAT3* and *NAT12* from *Arabidopsis thaliana*. Biochim Biophys Acta 1838: 3025–3035
1114 Nishimura K, van Wijk KJ (2015) Organization, function and substrates of the essential Clp
1115 protease system in plastids. Biochim Biophys Acta 1847: 915–930
1116 Oh E, Zhu J-Y, Bai M-Y, Arenhart RA, Sun Y, Wang Z-Y (2014) Cell elongation is regulated
1117 through a central circuit of interacting transcription factors in the Arabidopsis hypocotyl.
1118 Elife. doi: 10.7554/eLife.03031
1119 Ohashi-Ito K, Matsukawa M, Fukuda H (2013) An atypical bHLH transcription factor regulates
1120 early xylem development downstream of auxin. Plant Cell Physiol 54: 398–405
1121 Parsons RF (1968) The significance of growth-rate comparisons for plant ecology. Am Nat 102:
1122 595–597
1123 Páscoa P, Gouveia CM, Russo A, Trigo RM (2017) Drought Trends in the Iberian Peninsula over
1124 the Last 112 Years. Advances in Meteorology 2017: 1–13
1125 Picó FX (2012) Demographic fate of *Arabidopsis thaliana* cohorts of autumn- and spring-
1126 germinated plants along an altitudinal gradient. J Ecol 100: 1009–1018
1127 Picó FX, Méndez-Vigo B, Martínez-Zapater JM, Alonso-Blanco C (2008) Natural genetic variation
1128 of *Arabidopsis thaliana* is geographically structured in the Iberian peninsula. Genetics 180:
1129 1009–1021
1130 Pols AJ, Spahn A (2014) Biofuels: ethical issues. Encyclopedia of Food and Agricultural Ethics
1131 211–217
1132 Price AL, Zaitlen NA, Reich D, Patterson N (2010) New approaches to population stratification in
1133 genome-wide association studies. Nat Rev Genet 11: 459–463
1134 Rey Benayas JM, Scheiner SM (2002) Plant diversity, biogeography and environment in Iberia:
1135 Patterns and possible causal factors. J Veg Sci 13: 245
1136 Richards CL, Bossdorf O, Muth NZ, Gurevitch J, Pigliucci M (2006) Jack of all trades, master of
1137 some? On the role of phenotypic plasticity in plant invasions. Ecol Lett 9: 981–993
1138 Rober-Kleber N, Albrechtová JTP, Fleig S, Huck N, Michalke W, Wagner E, Speth V, Neuhaus G,
1139 Fischer-Iglesias C (2003) Plasma membrane H^+-ATPase is involved in auxin-mediated cell
1140 elongation during wheat embryo development. Plant Physiol 131: 1302–1312
1141 Running SW, Zhao M (2015) Daily GPP and annual NPP (MOD17A2/A3) products NASA Earth

1142 Observing System MODIS land algorithm. MOD17 User's Guide 2015: 1–28
1143 Salehin M, Li B, Tang M, Katz E, Song L, Ecker JR, Kliebenstein DJ, Estelle M (2019) Auxin-
1144 sensitive Aux/IAA proteins mediate drought tolerance in Arabidopsis by regulating
1145 glucosinolate levels. Nat Commun 10: 4021
1146 Sasaki E, Köcher T, Filiault DL, Nordborg M (2021) Revisiting a GWAS peak in *Arabidopsis*
1147 *thaliana* reveals possible confounding by genetic heterogeneity. BioRxiv. doi:
1148 10.1101/2021.02.03.429533
1149 Schär C, Vidale PL, Lüthi D, Frei C, Häberli C, Liniger MA, Appenzeller C (2004) The role of
1150 increasing temperature variability in European summer heatwaves. Nature 427: 332–336
1151 Schindele A, Dorn A, Puchta H (2020) CRISPR/Cas brings plant biology and breeding into the fast
1152 lane. Curr Opin Biotechnol 61: 7–14
1153 Schweizer F, Fernández-Calvo P, Zander M, Diez-Diaz M, Fonseca S, Glauser G, Lewsey MG,
1154 Ecker JR, Solano R, Reymond P (2013) Arabidopsis basic helix-loop-helix transcription
1155 factors MYC2, MYC3, and MYC4 regulate glucosinolate biosynthesis, insect performance,
1156 and feeding behavior. Plant Cell 25: 3117–3132
1157 Seren Ü, Vilhjálmsson BJ, Horton MW, Meng D, Forai P, Huang YS, Long Q, Segura V, Nordborg
1158 M (2012) GWAPP: a web application for genome-wide association mapping in Arabidopsis.
1159 Plant Cell 24: 4793–4805
1160 Siepielski AM, Morrissey MB, Buoro M, Carlson SM, Caruso CM, Clegg SM, Coulson T,
1161 DiBattista J, Gotanda KM, Francis CD, et al (2017) Precipitation drives global variation in
1162 natural selection. Science 355: 959–962
1163 Sohail M, Maier RM, Ganna A, Bloemendal A, Martin AR, Turchin MC, Chiang CW, Hirschhorn
1164 J, Daly MJ, Patterson N, et al (2019) Polygenic adaptation on height is overestimated due to
1165 uncorrected stratification in genome-wide association studies. Elife. doi:
1166 10.7554/eLife.39702
1167 Spartz AK, Ren H, Park MY, Grandt KN, Lee SH, Murphy AS, Sussman MR, Overvoorde PJ, Gray
1168 WM (2014) SAUR inhibition of PP2C-D Phosphatases activates plasma membrane H+-
1169 ATPases to promote cell expansion in arabidopsis. Plant Cell 26: 2129–2142
1170 Stortenbeker N, Bemer M (2019) The SAUR gene family: the plant's toolbox for adaptation of
1171 growth and development. J Exp Bot 70: 17–27
1172 Tabas-Madrid D, Méndez-Vigo B, Arteaga N, Marcer A, Pascual-Montano A, Weigel D, Xavier
1173 Picó F, Alonso-Blanco C (2018) Genome-wide signatures of flowering adaptation to climate
1174 temperature: regional analyses in a highly diverse native range of *Arabidopsis thaliana*.
1175 Plant Cell Environ 41: 1806–1820
1176 Takahashi K, Hayashi K, Kinoshita T (2012) Auxin activates the plasma membrane H+-ATPase by
1177 phosphorylation during hypocotyl elongation in Arabidopsis. Plant Physiol 159: 632–641
1178 Team RC (2013) R: A language and environment for statistical computing.
1179 The 1001 Genomes Consortium (2016) 1,135 Genomes reveal the global pattern of polymorphism
1180 in *Arabidopsis thaliana*. Cell 166: 481–491
1181 Tilman D (1988) Plant strategies and the dynamics and structure of plant communities. Princeton

1182 University Press
1183 Tunc-Ozdemir M, Tang C, Ishka MR, Brown E, Groves NR, Myers CT, Rato C, Poulsen LR,
1184 McDowell S, Miller G, et al (2013) A cyclic nucleotide-gated channel (CNGC16) in pollen
1185 is critical for stress tolerance in pollen reproductive development. Plant Physiol 161: 1010–
1186 1020
1187 Varvel GE, Vogel KP, Mitchell RB, Follett RF, Kimble JM (2008) Comparison of corn and
1188 switchgrass on marginal soils for bioenergy. Biomass and Bioenergy 32: 18–21
1189 Via S, Gomulkiewicz R, De Jong G, Scheiner SM, Schlichting CD, Van Tienderen PH (1995)
1190 Adaptive phenotypic plasticity: consensus and controversy. Trends Ecol Evol (Amst) 10:
1191 212–217
1192 Vicente-Serrano SM (2006a) Spatial and temporal analysis of droughts in the Iberian Peninsula
1193 (1910–2000). Hydrological Sciences Journal 51: 83–97
1194 Vicente-Serrano SM (2006b) Differences in spatial patterns of drought on different time scales: an
1195 analysis of the iberian peninsula. Water Resour Manage 20: 37–60
1196 Vidigal DS, Marques ACSS, Willems LAJ, Buijs G, Méndez-Vigo B, Hilhorst HWM, Bentsink L,
1197 Picó FX, Alonso-Blanco C (2016) Altitudinal and climatic associations of seed dormancy
1198 and flowering traits evidence adaptation of annual life cycle timing in *Arabidopsis thaliana*.
1199 Plant Cell Environ 39: 1737–1748
1200 Waddington CH (1953) Genetic assimilation of an acquired character. Evolution 7: 118
1201 Wang Y-F, Munemasa S, Nishimura N, Ren H-M, Robert N, Han M, Puzõrjova I, Kollist H, Lee S,
1202 Mori I, et al (2013) Identification of cyclic GMP-activated nonselective Ca2+-permeable
1203 cation channels and associated CNGC5 and CNGC6 genes in Arabidopsis guard cells. Plant
1204 Physiol 163: 578–590
1205 Wang Z, Yang L, Liu Z, Lu M, Wang M, Sun Q, Lan Y, Shi T, Wu D, Hua J (2019) Natural
1206 variations of growth thermo-responsiveness determined by SAUR26/27/28 proteins in
1207 *Arabidopsis thaliana*. New Phytol 224: 291–305
1208 Wang Z, Yang L, Wu D, Zhang N, Hua J (2021) Polymorphisms in cis-elements confer SAUR26
1209 gene expression difference for thermo-response natural variation in Arabidopsis. New
1210 Phytol 229: 2751–2764
1211 Waters BM, Chu H-H, Didonato RJ, Roberts LA, Eisley RB, Lahner B, Salt DE, Walker EL (2006)
1212 Mutations in Arabidopsis yellow stripe-like1 and yellow stripe-like3 reveal their roles in
1213 metal ion homeostasis and loading of metal ions in seeds. Plant Physiol 141: 1446–1458
1214 West-Eberhard MJ (2003) Developmental plasticity and evolution. Oxford University Press
1215 Wickham H, Francois R, Henry L, Müller K (2015) dplyr: A grammar of data manipulation. R
1216 package version 0.4 3:
1217 Wickham H, Henry L (2018) tidyr: Easily Tidy Data with ‘spread ()’and ‘gather ()’Functions. R
1218 package version 0.8 2:
1219 Wolfe MD, Tonsor SJ (2014) Adaptation to spring heat and drought in northeastern Spanish
1220 *Arabidopsis thaliana*. New Phytol 201: 323–334
1221 Yamori W, Sakata N, Suzuki Y, Shikanai T, Makino A (2011) Cyclic electron flow around

1222 photosystem I via chloroplast NAD(P)H dehydrogenase (NDH) complex performs a
1223 significant physiological role during photosynthesis and plant growth at low temperature in
1224 rice. Plant J 68: 966–976
1225 Zhang H, Zhao Y, Zhu J-K (2020) Thriving under stress: how plants balance growth and the stress
1226 response. Dev Cell 55: 529–543
1227 Zhang J, Vankova R, Malbeck J, Dobrev PI, Xu Y, Chong K, Neff MM (2009) *AtSOFL1* and
1228 *AtSOFL2* act redundantly as positive modulators of the endogenous content of specific
1229 cytokinins in Arabidopsis. PLoS One 4: e8236
1230 Zheng Q, Zheng Y, Ji H, Burnie W, Perry SE (2016) Gene regulation by the *AGL15* transcription
1231 factor reveals hormone interactions in somatic embryogenesis. Plant Physiol 172: 2374–
1232 2387
1233 Zhiponova MK, Morohashi K, Vanhoutte I, Machemer-Noonan K, Revalska M, Van Montagu M,
1234 Grotewold E, Russinova E (2014) Helix-loop-helix/basic helix-loop-helix transcription
1235 factor network represses cell elongation in Arabidopsis through an apparent incoherent feed-
1236 forward loop. Proc Natl Acad Sci USA 111: 2824–2829
1237

A

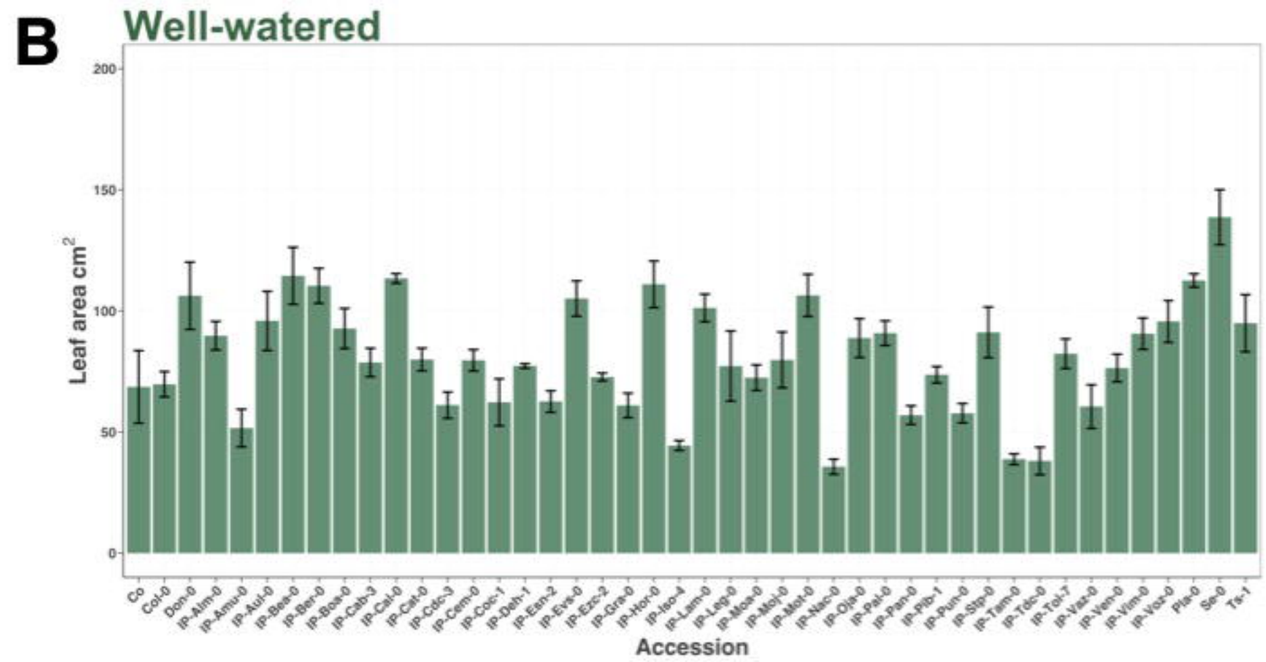
B
Well-watered
Leaf area cm^2
Accession

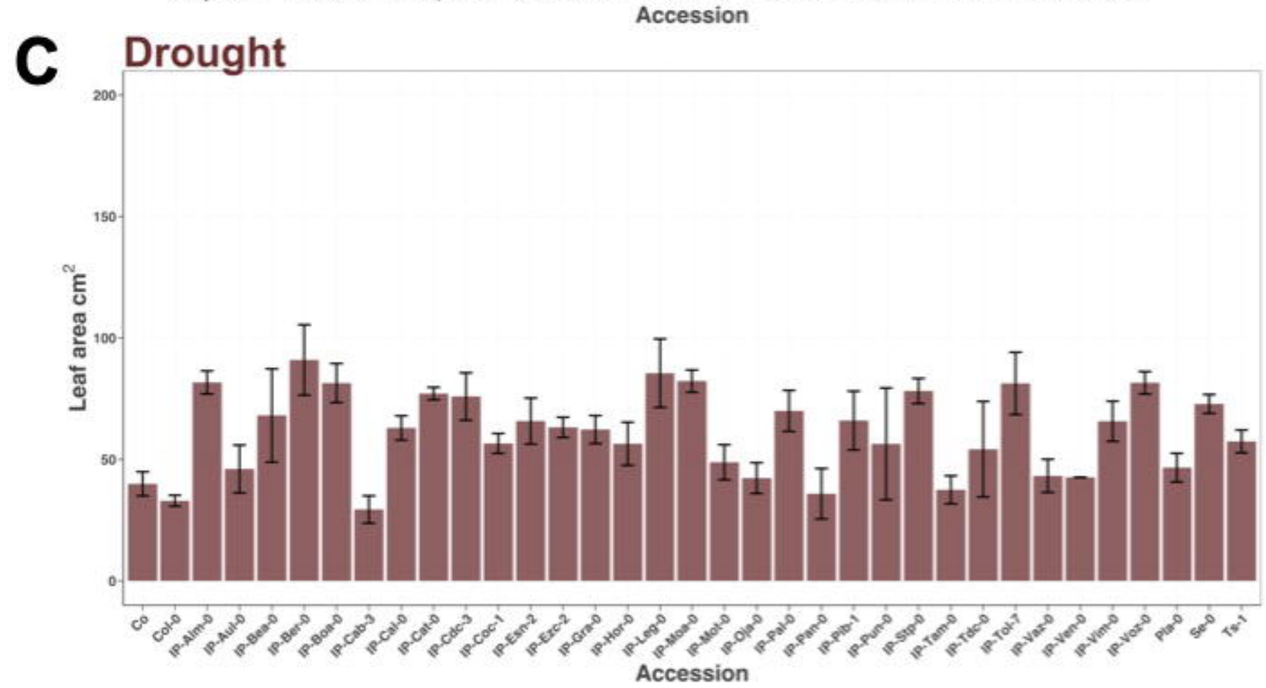
C
Drought
Leaf area cm^2
Accession

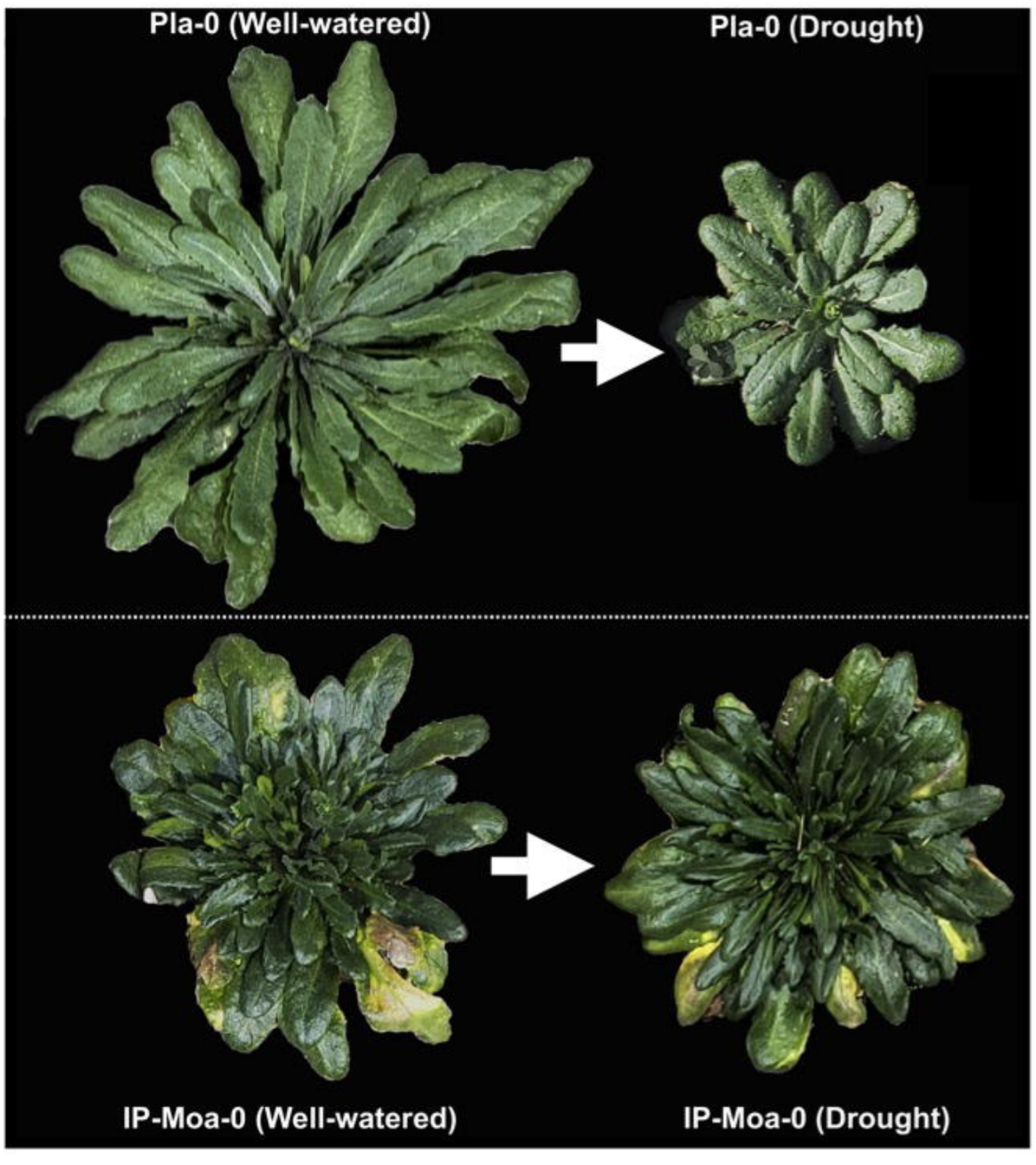
D
Pla-0 (Well-watered)
Pla-0 (Drought)
IP-Moa-0 (Well-watered)
IP-Moa-0 (Drought)

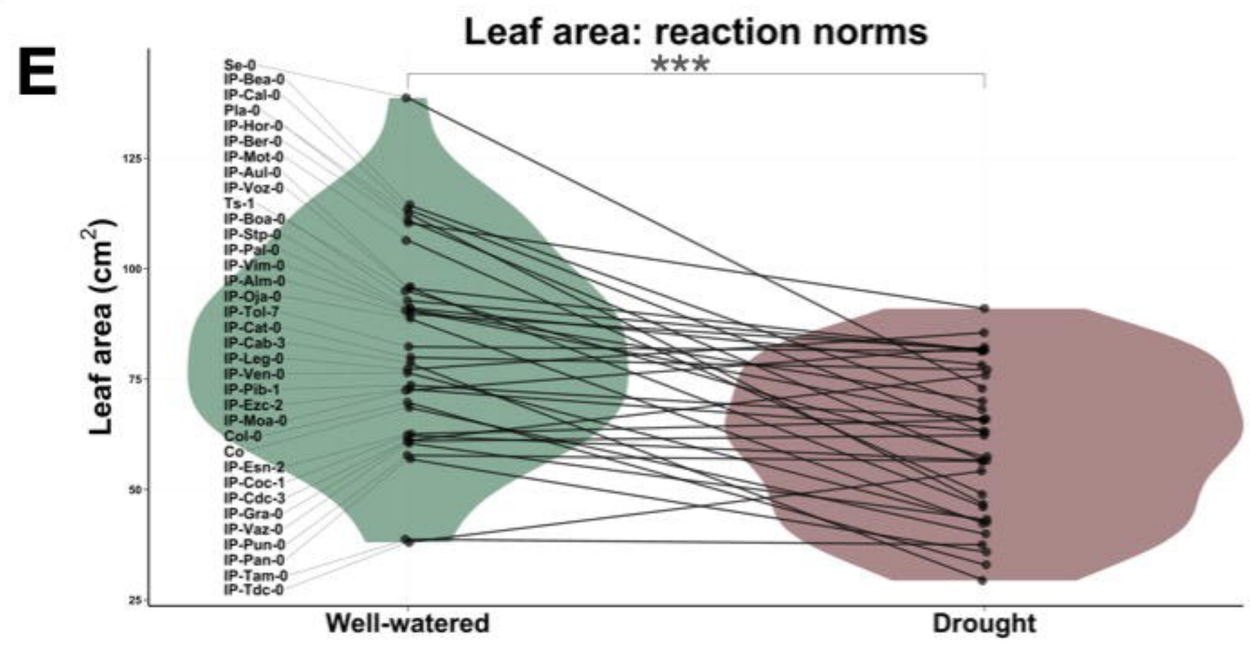
E
Leaf area: reaction norms
***
Leaf area (cm^2)
Well-watered
Drought

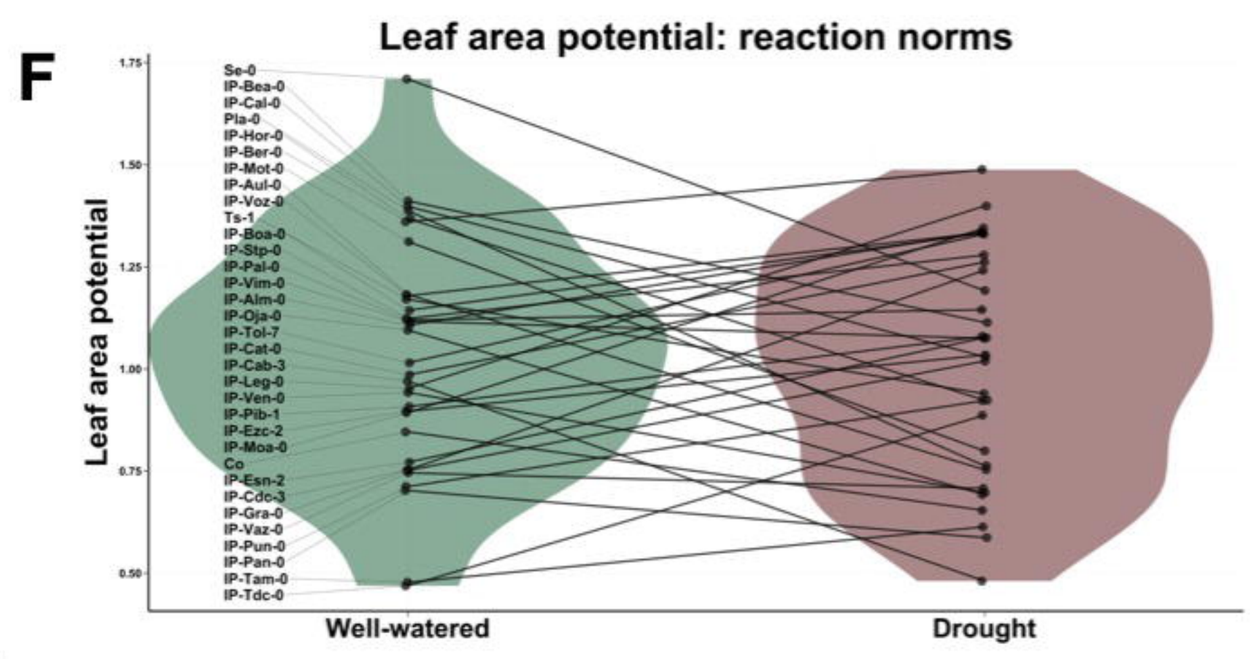
F
Leaf area potential: reaction norms
Leaf area potential
Well-watered
Drought

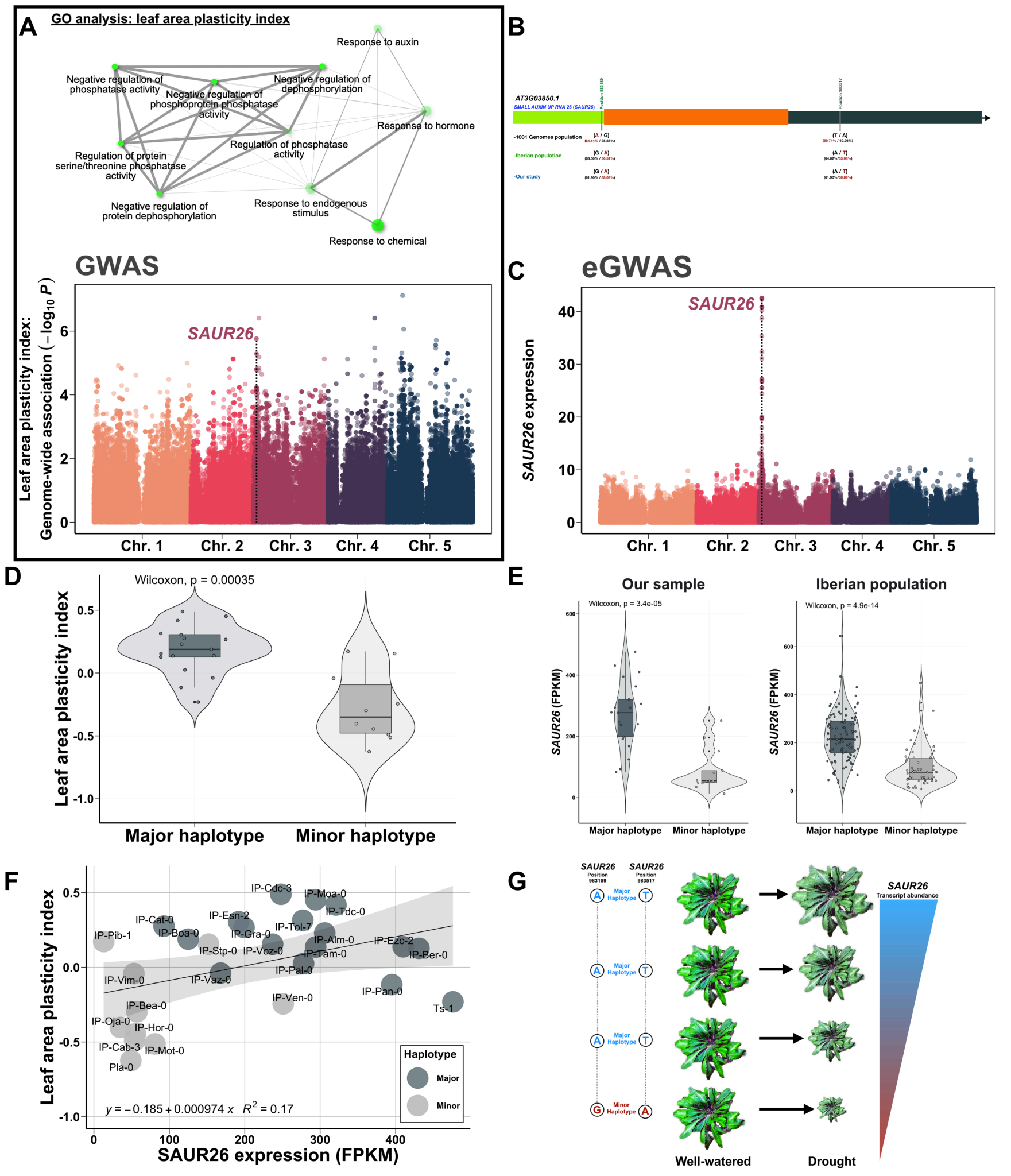
A
GO analysis: leaf area plasticity index
Response to auxin
Negative regulation of phosphatase activity
Negative regulation of dephosphorylation
Negative regulation of phosphoprotein phosphatase activity
Response to hormone
Regulation of phosphatase activity
Regulation of protein serine/threonine phosphatase activity
Negative regulation of protein dephosphorylation
Response to endogenous stimulus
Response to chemical
B
AT3G03850.1
SMALL AUXIN UP RNA 26 (SAUR26)
Position 983189
Position 983517
-1001 Genomes population
(A / G)
(64.14% / 35.85%)
(T / A)
(59.74% / 40.26%)
-Iberian population
(G / A)
(63.50% / 36.51%)
(A / T)
(64.02%/35.98%)
-Our study
(G / A)
(61.90% / 38.09%)
(A / T)
(61.90%/38.09%)
GWAS
Leaf area plasticity index: Genome-wide association (−log10 P)
SAUR26
Chr. 1
Chr. 2
Chr. 3
Chr. 4
Chr. 5
C
eGWAS
SAUR26 expression
SAUR26
Chr. 1
Chr. 2
Chr. 3
Chr. 4
Chr. 5
D
Wilcoxon, p = 0.00035
Leaf area plasticity index
Major haplotype
Minor haplotype
E
Our sample
Wilcoxon, p = 3.4e-05
Iberian population
Wilcoxon, p = 4.9e-14
SAUR26 (FPKM)
Major haplotype
Minor haplotype
F
Leaf area plasticity index
SAUR26 expression (FPKM)
IP-Cdc-3
IP-Moa-0
IP-Tdc-0
IP-Cat-0
IP-Esn-2
IP-Tol-7
IP-Pib-1
IP-Boa-0
IP-Gra-0
IP-Alm-0
IP-Ezc-2
IP-Stp-0
IP-Voz-0
IP-Tam-0
IP-Ber-0
IP-Pal-0
IP-Vim-0
IP-Vaz-0
IP-Pan-0
IP-Ven-0
IP-Bea-0
Ts-1
IP-Oja-0
IP-Hor-0
IP-Cab-3
IP-Mot-0
Pla-0
Haplotype
Major
Minor
y = −0.185 + 0.000974 x R2 = 0.17
G
SAUR26 Position 983189
SAUR26 Position 983517
Major Haplotype
Minor Haplotype
SAUR26
Transcript abundance
Well-watered
Drought

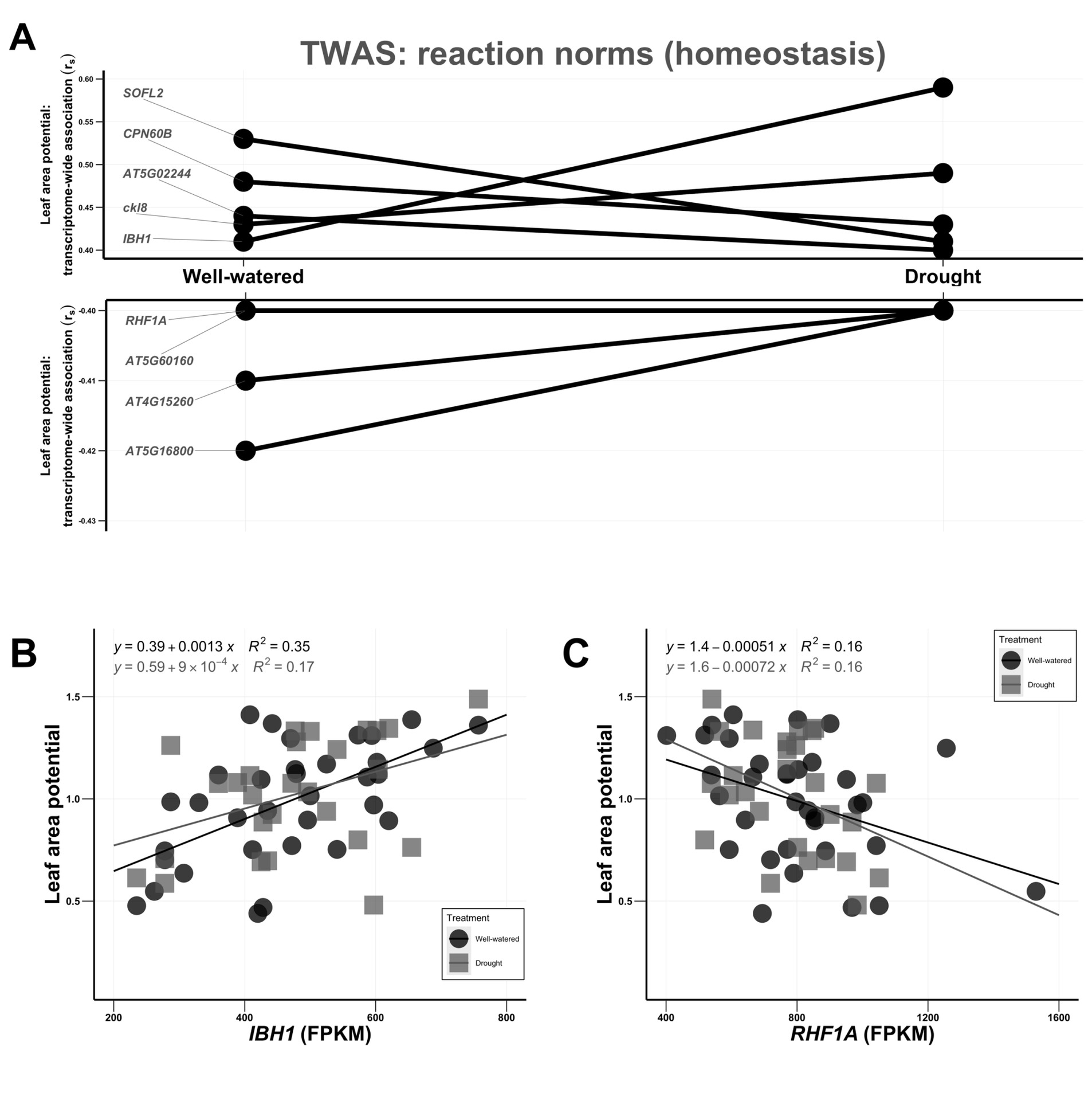
A
TWAS: reaction norms (homeostasis)
Leaf area potential: transcriptome-wide association (r_s)
0.60
0.55
0.50
0.45
0.40
SOFL2
CPN60B
AT5G02244
ckl8
IBH1
Well-watered
Drought
-0.40
-0.41
-0.42
-0.43
RHF1A
AT5G60160
AT4G15260
AT5G16800
B
$y = 0.39 + 0.0013\,x$ $R^2 = 0.35$
$y = 0.59 + 9 \times 10^{-4}\,x$ $R^2 = 0.17$
Leaf area potential
1.5
1.0
0.5
200
400
600
800
IBH1 (FPKM)
Treatment
Well-watered
Drought
C
$y = 1.4 - 0.00051\,x$ $R^2 = 0.16$
$y = 1.6 - 0.00072\,x$ $R^2 = 0.16$
Leaf area potential
1.5
1.0
0.5
400
800
1200
1600
RHF1A (FPKM)
Treatment
Well-watered
Drought

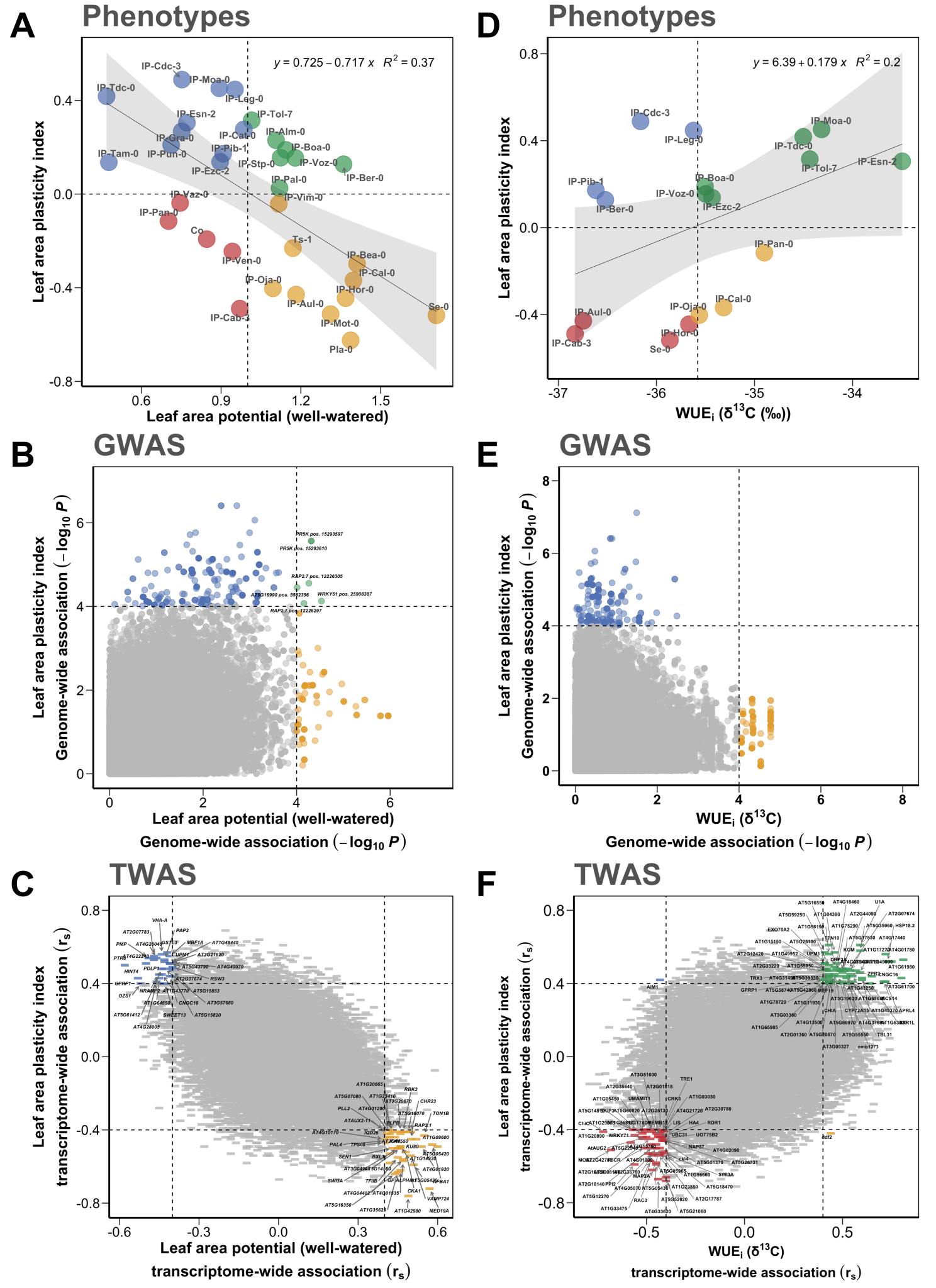
A
Phenotypes
y = 0.725 – 0.717 x R2 = 0.37
Leaf area plasticity index
Leaf area potential (well-watered)
D
Phenotypes
y = 6.39 + 0.179 x R2 = 0.2
Leaf area plasticity index
WUEi (δ13C (‰))
B
GWAS
Leaf area plasticity index
Genome-wide association (–log10 P)
Leaf area potential (well-watered)
Genome-wide association (–log10 P)
E
GWAS
Leaf area plasticity index
Genome-wide association (–log10 P)
WUEi (δ13C)
Genome-wide association (–log10 P)
C
TWAS
Leaf area plasticity index
transcriptome-wide association (rs)
Leaf area potential (well-watered)
transcriptome-wide association (rs)
F
TWAS
Leaf area plasticity index
transcriptome-wide association (rs)
WUEi (δ13C)
transcriptome-wide association (rs)

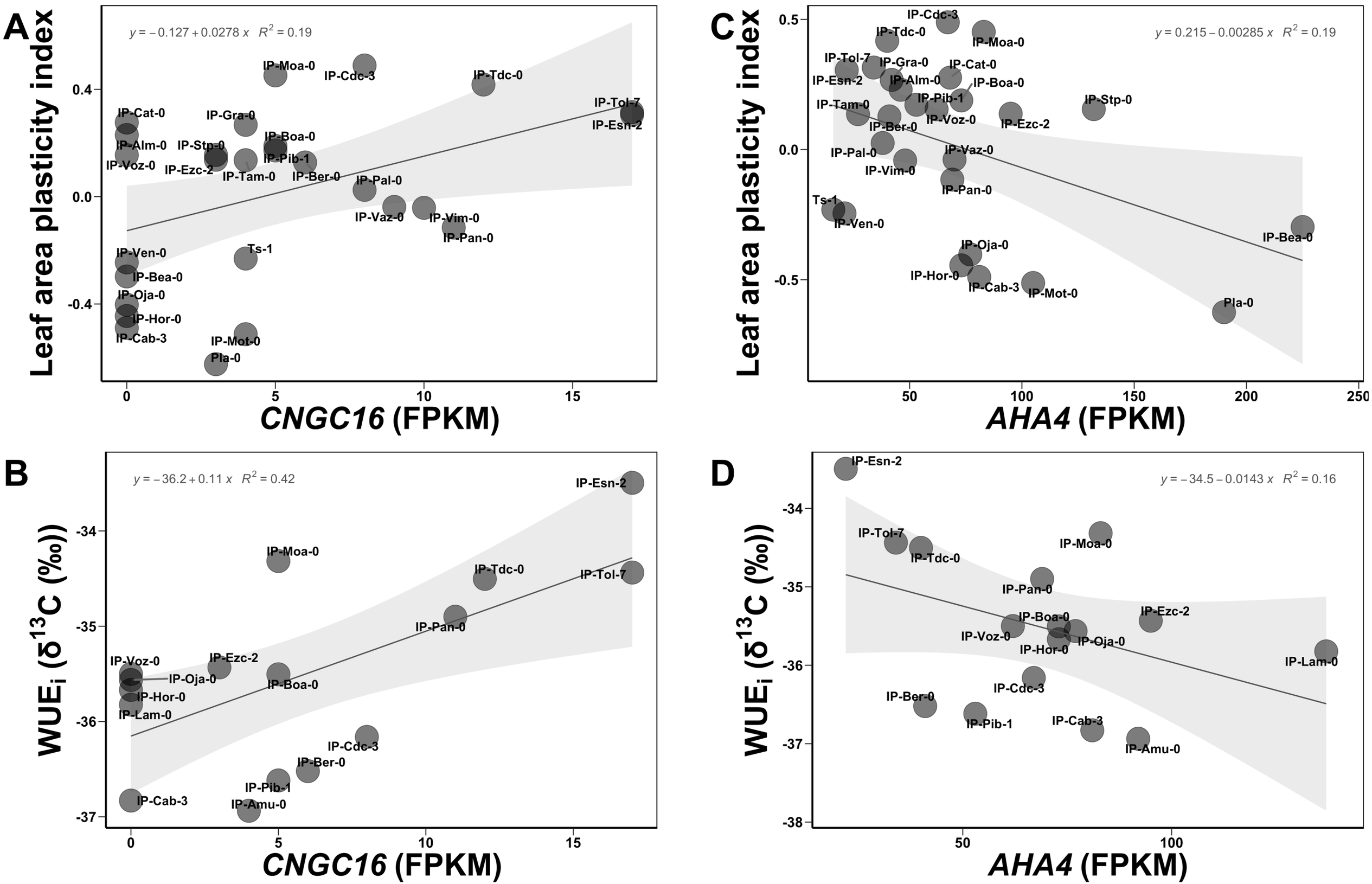
A
y = −0.127 + 0.0278 x R² = 0.19
Leaf area plasticity index
CNGC16 (FPKM)
IP-Moa-0
IP-Cdc-3
IP-Tdc-0
IP-Tol-7
IP-Esn-2
IP-Cat-0
IP-Gra-0
IP-Boa-0
IP-Alm-0
IP-Stp-0
IP-Pib-1
IP-Voz-0
IP-Ezc-2
IP-Tam-0
IP-Ber-0
IP-Pal-0
IP-Vaz-0
IP-Vim-0
IP-Pan-0
Ts-1
IP-Ven-0
IP-Bea-0
IP-Oja-0
IP-Hor-0
IP-Cab-3
IP-Mot-0
Pla-0
B
y = −36.2 + 0.11 x R² = 0.42
WUEi (δ13C (‰))
CNGC16 (FPKM)
C
y = 0.215 − 0.00285 x R² = 0.19
Leaf area plasticity index
AHA4 (FPKM)
D
y = −34.5 − 0.0143 x R² = 0.16
WUEi (δ13C (‰))
AHA4 (FPKM)

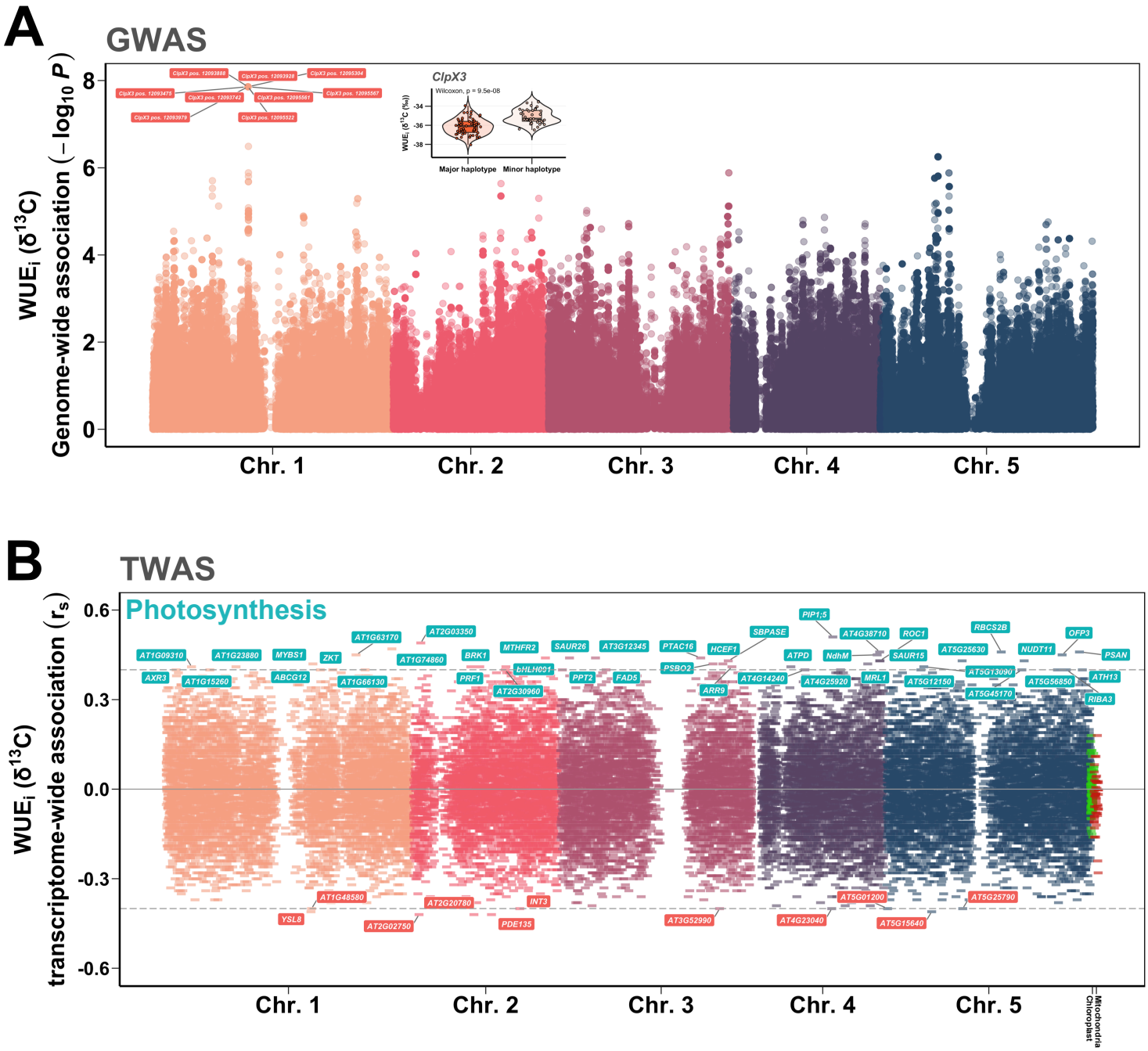
A
GWAS
Genome-wide association (−log10 P)
WUEi (δ13C)
ClpX3
Wilcoxon, p = 9.5e-08
Major haplotype
Minor haplotype
Chr. 1
Chr. 2
Chr. 3
Chr. 4
Chr. 5
B
TWAS
Photosynthesis
transcriptome-wide association (rs)
WUEi (δ13C)
Mitochondria
Chloroplast

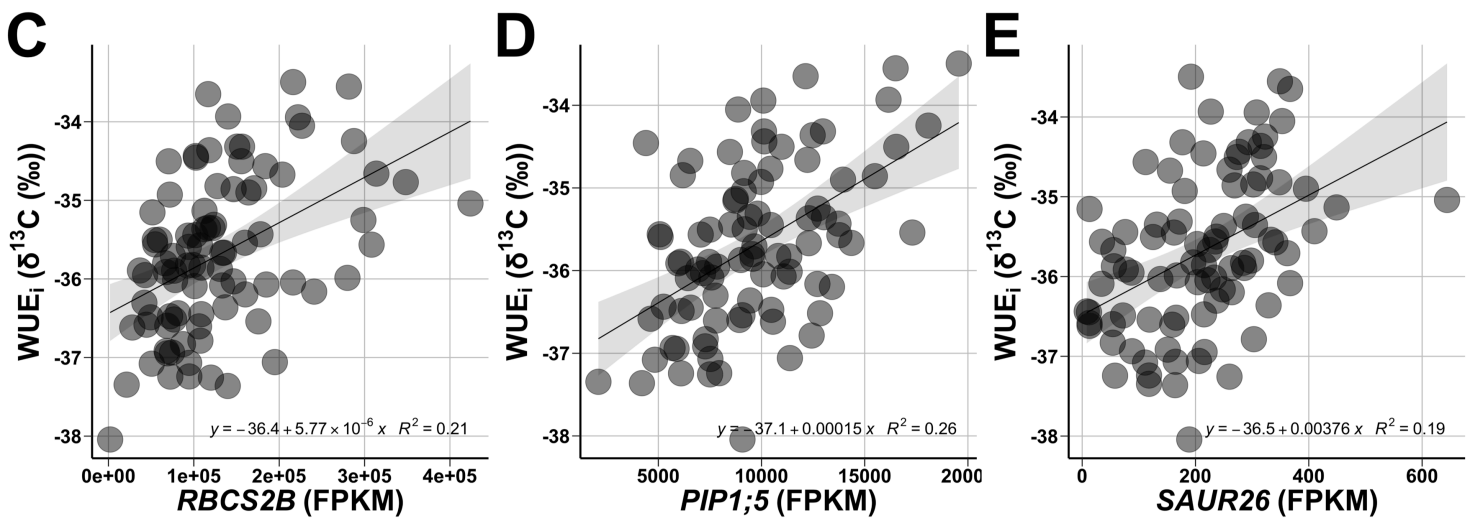
C
D
E
WUEi (δ13C (‰))
y = −36.4 + 5.77 × 10−6 x R2 = 0.21
RBCS2B (FPKM)
y = −37.1 + 0.00015 x R2 = 0.26
PIP1;5 (FPKM)
y = −36.5 + 0.00376 x R2 = 0.19
SAUR26 (FPKM)